



Available online at www.sciencedirect.com

ScienceDirect

Advances in Space Research 62 (2018) 2026–2045

**ADVANCES IN
SPACE
RESEARCH**
(*a COSPAR publication*)
www.elsevier.com/locate/asr

Low-thrust tour of the main belt asteroids

Marilena Di Carlo, Massimiliano Vasile, Jamie Dunlop

Department of Mechanical and Aerospace Engineering, University of Strathclyde, 75 Montrose Street, G1 1XJ Glasgow, United Kingdom

Received 13 March 2017; received in revised form 12 December 2017; accepted 14 December 2017

Available online 4 January 2018

Abstract

This work presents some initial results on a possible low-thrust tour of the main asteroid belt. The asteroids are visited through a series of fly-by's to be completed within a given time-frame and limit on the mass of the spacecraft at launch. The asteroids to be visited are automatically selected out of a large database of possible candidates. The initial shortlist of targets is based on the Minimum Orbit Intersection Distance (MOID) between the orbit of the asteroids in the database and the initial orbit of the spacecraft traversing the main belt. The final sequence is then obtained with an efficient deterministic branch and prune algorithm. The transfers between asteroids are designed using a low-thrust analytical model that provides a good estimation of the propellant consumption and transfer time. The mission analysis is completed with a study of the cost of the launch. In this paper two databases will be analysed: one containing only targets with a particular scientific relevance and one containing all available asteroids.

© 2018 COSPAR. Published by Elsevier Ltd. All rights reserved.

Keywords: Main asteroid belt; Low-thrust mission

1. Introduction

The main belt houses the majority of the asteroids in the Solar System. It extends from 2.1 AU to 4 AU (Minton et al. (2009)) and is estimated to contain several million asteroids, ranging in size from few millimeters to the 959 km diameter of Ceres (Millis et al., 1987). Although larger asteroid are observable from Earth and are easy to identify, the classification of smaller objects still remains an open problem. Furthermore, there is an interest in a characterisation of the larger ones to better understand their composition and evolution from the primordial stages of the Solar System till now. Key information on the composition of objects in the main belt can only be obtained from space-based spectroscopy and close encounter analysis (Bowles et al., 2018). A mission that could visit at least ten objects

will double the number of asteroids visited to date. However, designing a mission to characterise that many asteroids in the main belt is not an easy task. The main difficulty is to identify long sequences of asteroids that can be visited in a given time and with limited ΔV . The number of known objects exceeds 641,933 ¹ and the number of possible combinations of encounter is unmanageable.

The mission currently targeting objects in the main belt, Dawn,² is visiting only two proto-planets using low-thrust propulsion. After visiting Vesta in 2011–2013 (Rayman and Mase, 2014), Dawn is now exploring the dwarf planet Ceres (Russell et al., 2016).

Examples of previous works on the design of asteroid tours divided the design process into different steps (Olympio, 2011): the first step consists in the definition of a shortlist of potential targets, based on their orbital

E-mail addresses: marilena.di-carlo@strath.ac.uk (M. Di Carlo), massimiliano.vasile@strath.ac.uk (M. Vasile), jamie.dunlop.2013@uni.strath.ac.uk (J. Dunlop)

¹ http://ssd.jpl.nasa.gov/sbdb_query.cgi#x.

² <http://dawn.jpl.nasa.gov/>.

elements, dimensions or scientific characteristics. In the second step a sequence of target objects is selected using some form of global optimisation (Alemany et al., 2007) in combination with reduced models that provide a quick estimation of the cost of the transfer. The last step is the optimisation of the sequence with a local optimisation method. A recent work by Cuartielles et al. (2016) proposes a mission to fly-by 10 or more asteroids in 7 years in the timeframe 2029–2030, using a spacecraft equipped with a chemical engine launched by a Soyuz launcher. The study includes the possible use of a gravity assist of Mars. A branch and bound search method is used to identify an optimal sequence of asteroids under the assumption that all fly-by's with the asteroids occur at the point of Minimum Orbital Intersection Distance (MOID). The use of gravity assist to reach the main belt is studied also by Chen et al. (2014), who present the results of an analysis of accessibility for 200 asteroids in the main belt with diameter greater than 100 km. The global minimum of the cost of the transfer to these asteroids, using gravity assists with Mars or Earth, is sought. Results show that Mars is the most useful gravity-assist body and that dual gravity assists with Mars are the best type of trajectories to reach mid or outer belt asteroids and high-inclination ones. The low-thrust transfer to asteroid Flora is included in the analysis. The control profile for the low-thrust transfer is optimised with an indirect optimal control method and homotopy. Shang and Liu (2017) proposed a machine learning method based on Gaussian Process Regressions to study the accessibility of more than 600,000 main belt asteroids considering rendezvous realised through bi-impulsive or Mars gravity-assisted transfers. Mars' gravity assists to reach the main belt are also proposed by Yang et al. (2015). In this work, the transfer from a near-Earth asteroid to a main belt asteroid, using low-thrust propulsion and multiple gravity assists, is studied. Based on an analysis of the Tisserand graph, the Earth-Mars-Mars gravity assists sequence is found to be the best option to reach the main belt. A global solver is then used to obtain the event dates for the gravity assists and the deep space manoeuvres, using an impulsive model for the transfers. Finally, the optimal control problem for the design of the low-thrust trajectory is solved using an indirect method and homotopy.

In recent times, the problem of visiting multiple asteroids was part of the objective of some Global Trajectory Optimisation Competitions (GTOC).³ In particular, in GTOC4 the problem was to identify the maximum number of asteroids' fly-bys from a given list of 1438 objects, considering a rendezvous with the last asteroid in the sequence and a total mission time of ten years. GTOC5 also proposed a mission to Near Earth Asteroids (NEAs) (Bottke et al., 2000; Stuart, 2001), considering a database of 7073 objects, while GTOC7 presented a multi-spacecraft exploration of the asteroid belt

and a database of 16,256 potential targets. For GTOC4, the first ranking team found a solution visiting 44 asteroids (Grigoriev and Zapletin, 2013). They solved the discrete part of the problem (the identification of the optimal sequence of asteroids to visit) using dynamic programming, performing the construction of the solution vector step by step and optimising time and mass consumption at each step. The trajectory was approximated with a solution of the Lambert problem. Lantoine and Russell (2012) used an algorithm called HDDP (Hybrid Differential Dynamic Programming), a variant of the classical Differential Dynamic Programming technique. The multi-phase formulation of HDDP was used by splitting the trajectory into several portions connected by the fly-by's at the asteroids. The initial guess was obtained from a ballistic Lambert solution that provided the asteroid sequence. The solution was characterised by 24 fly-by's and 1 rendezvous.

This paper presents some results for a possible tour of the main asteroid belt using solar electric propulsion. The particular problem presented in this paper is similar to the one proposed in Cuartielles et al. (2016) and differs from previous analyses of the accessibility of the main belt or asteroid tours considered in past GTOCs. More specifically, in order to limit mission time and total mass at launch, the strategy proposed in this paper is to fly-by as many asteroids as possible at their nodal points by traversing the asteroid belt with an elliptical orbit with perihelion at (or near) the Earth and aphelion at the main belt. Each asteroid is expected to be visited with one single fly-by only (see Di Carlo et al. (2017b) and Vroom et al. (2016)). The resulting combinatorial problem is solved with a combination of two simple pruning techniques over the space of possible fly-by's. The first pruning is on the MOID between the initial orbit and the asteroids in the database. After this first pruning a deterministic branch and prune algorithm is applied to a binary tree that incrementally constructs the optimal sequence of targets. Finally, the best solution is re-optimised with electric propulsion. A direct transcription method based on asymptotic analytical solutions to the accelerated Keplerian motion (Zuiani et al., 2012) is used to transcribe the optimal control problem that defines the optimal control profile of the engine. The transfer from the Earth to the initial elliptical orbit traversing the main belt is then optimised with the same transcription approach.

The length of the tour is constrained by a given total mission time and desirable launch capability. Two scenarios are considered: in the first scenario the database of target objects includes scientifically interesting bodies and tries to find the longest sequence of objects in a given time and ΔV budgets; in the second scenario, more than 100,000 objects are added to the previous database and the aim is to find the longest sequence of asteroids that contains also some (more than 0) scientifically interesting targets. Note that the number of possible targets is, in this case, about one order of magnitude larger than the one of previous GTOCs. The analysis proceeds, as in the first

³ https://sophia.estec.esa.int/gtoc_portal/.

scenario, with the study of all optimal sequences that are achievable with a given time limit and ΔV budget.

In this paper we limit our attention to transfer options that do not include swing-by's of the inner planets of the solar system; this reduces the complexity of the mission and improve the flexibility of the launch window. The transfer from the Earth to the main belt is, instead, conceived to exploit at best the use of the launcher and the electric propulsion system. The launch feasibility, using two possible launchers, is also studied.

The paper is structured as follows: the proposed solution method to define a mission to the main belt is presented in Section 2. The results are then presented in Sections 3 and 4, and Section 5 concludes the paper.

2. Mission analysis

In this work two databases of objects in the main belt are considered. The first database (Database 1) includes a selection of 424 objects of particular scientific interest (the database was kindly provided by the PI of the CAST-Away mission proposal⁴). These are, among others, active objects (main belt comets, mass losing asteroids), objects of extreme sizes (both small and big) and extreme shapes, fast rotators, binaries or triples and asteroid pairs. The second database (Database 2) is composed of 101,993 objects (Cuartielles et al., 2016). The distribution of semimajor axis a , eccentricity e and inclination i of the objects of the two databases is shown in Figs. 1 and 2, where the curve $q = Q_{\text{Mars}}$ identifies the values of a and e such that the perihelion q is equal to the aphelion of Mars Q_{Mars} while $Q = q_{\text{Jup}}$ identifies the values of a and e such that the aphelion Q is equal to the perihelion of Jupiter. Note that, although the complete Database 2 contains also asteroids with perihelion at Jupiter, in this analysis we will restrict our attention to asteroids that are part of the main belt.

The approach taken in this paper to design the tour of the asteroid belt is conceptually analogous to the one proposed by the authors in previous work (see Di Carlo et al., 2017b) and formulates the underlying trajectory design problem in the same fashion as in Cuartielles et al. (2016). The idea is to traverse the asteroid belt with a high elliptical orbit and to encounter as many asteroids as possible at their nodal points to avoid any plane change. Thus the orbit of the spacecraft is designed to be in the ecliptic plane and electric propulsion is used to modify the elliptical orbit enough to obtain the required fly-by distance. Different planes could potentially increase the length of the sequence of encounters though it would incur in an additional ΔV . The use of one or more swing-by's of the inner planets could mitigate this problem and increase both aphelion and perihelion but also increase the operational complexity of the mission. Therefore, the analysis in this paper will be limited to the case in which no swing-by's

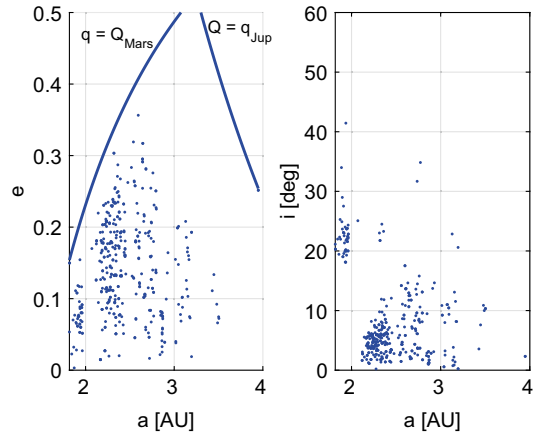


Fig. 1. a - e and a - i distribution of the selected objects in the main belt for Database 1.

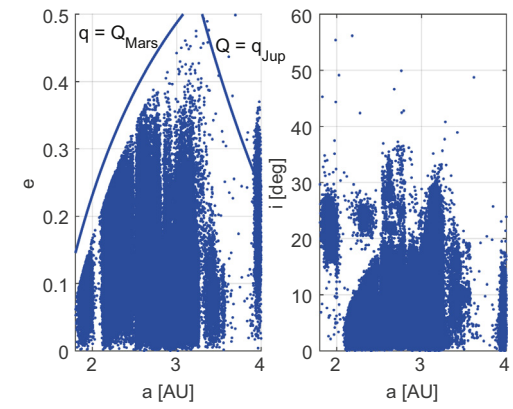


Fig. 2. a - e and a - i distribution of the selected objects in the main belt for Database 2.

are introduced and the orbit of the spacecraft remains in the ecliptic plane.

The tour of the main belt is assumed to start on the 01/01/2030 with a maximum duration of 5 years to limit operations and respond to the requirements and scientific objectives of CASTAway. The spacecraft is injected in a heliocentric orbit exploiting the C_3 provided by the launcher and then uses the electric engine to achieve the desired elliptical orbit. Note that other dates around the 01/01/2030 were analysed but it was found that the 01/01/2030 was optimal, thus this paper will present only the results for the 01/01/2030 as they are the most significant ones (Section 4.2).

The overall approach can be conceptually divided in five steps that are briefly introduced in the following and described in more details in the next subsections:

1. Analysis of the MOID between different possible initial orbits of the spacecraft traversing the main belt and the orbits of all the asteroids in the database (Section 2.1). This is a natural step to shortlist groups of asteroids that can be easily reached with a fly-by within the desired time frame. Note that the idea of using the MOID

⁴ <https://sites.google.com/site/castawaymission/>.

- descends from the idea of traversing the main belt with a high elliptical orbit.
2. Definition of the sequence of asteroid close encounters starting from the shortlist derived from step 1. The MOIDs in the shortlist might be excessively big to allow achieving the scientific goals of the mission, therefore, the elliptical orbit needs to be modified to guarantee an appropriate distance from each asteroid. Such a modification incurs in an additional ΔV cost that needs to be traded-off against the number of close encounters (Section 2.2). For this step we use a multi-impulse model and a simple but effective binary decision tree coupled with a deterministic branch and prune approach.
 3. Optimisation of the parameters of the initial orbit in the main belt, of the times of the impulsive maneuvers and of the times of the encounters with the asteroids to reduce the ΔV associated with the tour (Section 2.3). This step, although not strictly required, provides an optimised impulsive solution that can be used as it is or recalculated considering an electric propulsion engine.
 4. Study of the transfer from the Earth to the main belt (Section 2.4).
 5. Optimisation of the low-thrust transfer to the main belt and of the tour of the selected sequence of asteroids (Section 2.5). For this step we used a novel transcription method that was already demonstrated to be fast and effective and to provide conservative but good estimations of the total mass budget.

The analysis of the transfer to the main belt and of the encounter sequence is then completed by a launch sequence analysis to assess which launch system can be used for this particular mission.

2.1. Minimum orbit intersection distance

In order to identify the initial orbit of the spacecraft and shortlist the asteroids to encounter, the MOID (Gronchi, 2002, 2005) between all the asteroids in the database and different possible initial orbits of the spacecraft is computed. The MOID is defined as a measure for the distance between the orbits of two objects. The computation of the MOID is realised using the Fortran code publicly available online from the Department of Mathematics of the University of Pisa, Italy.⁵ This computation returns, for each pair spacecraft's orbit-asteroids's orbit, the minimum, maximum and saddle points of the distance between the two orbits. These critical points are identified by the true anomalies θ_{ast}^{MOID} and θ_{sc}^{MOID} of the two objects on their orbit and by the distance between them at the critical points, d . In this study only points with $d < 0.01$ AU are considered. The computation of the MOID does not consider, however, the positions that the asteroids and spacecraft occupy

on their orbits (Bonanno, 2000). This means that an encounter between spacecraft and asteroid cannot actually take place if the two bodies are not, at the same time, at θ_{ast}^{MOID} and θ_{sc}^{MOID} . In order to check which encounters at the MOID can be actually be realised, the following phasing analysis is applied:

- For each couple spacecraft's orbit – asteroid's orbit with $d < 0.01$ AU, the times when the asteroid is at θ_{ast}^{MOID} are computed, starting from the initial date 01/01/2030, $t_0 = 10957.5$ MJD2000. These times, that repeat at intervals equal to the orbital period of the asteroid, are identified as T_{ast}^{MOID} .
- Different initial mean anomalies M_0 in the range [0, 360) deg, at steps of 1 deg, are considered for the spacecraft on its orbit, with initial date t_0 .
- Kepler equation is solved to obtain the true anomaly of the spacecraft at $T_{sc}^{MOID}, \theta_{sc}(T_{sc}^{MOID})$, starting from M_0 at t_0 . If the following condition is satisfied

$$|\theta_{sc}(T_{sc}^{MOID}) - \theta_{sc}^{MOID}| < \delta \quad (1)$$

then the encounter between asteroid and spacecraft, at distance $d < 0.01$ AU, actually takes place at time T_{sc}^{MOID} . δ is an appropriate small angle.

2.2. Study of the possible sequences of asteroids

At the end of the process defined in the previous subsection, for each value of M_0 (angular position of the spacecraft on the initial orbit at time t_0), a list of asteroids that the spacecraft encounters at a distance lower than 0.01 AU is available. The next step consists in computing the ΔV required to fly-by these objects. The cost of the transfer between one asteroid and the next is computed with a Lambert solver (Vallado, 2007). The total cost is given by the sum of all the ΔV_i , $\Delta V = \sum_i \Delta V_i$. Encountering each asteroid in the sequence could be however too expensive in terms of ΔV . This study, therefore, tries to identify a subset of objects, in the list of asteroids, that can be visited with a cost lower than a maximum allowable total ΔV_{max} budget. In order to do so, for a sequence of n asteroids, a vector \mathbf{b} of length n composed of 0's and 1's is defined to identify which asteroids are encountered (1) and which ones are not (0). As a result, 2^n sequences, each characterised by a different number of asteroids and different values of ΔV , are available and need to be evaluated. An enumerative approach to evaluate all the 2^n possibilities is not practical when n is large. Thus a deterministic Branch and Prune Approach (BPA) is applied. The BPA incrementally builds a binary tree in which each level corresponds to one of the n components in \mathbf{b} and each branch is a sequence. At each level each branch is divided in two sub-branches, one with leaf with value 1 and one with leaf with value 0. Then each partial branch is evaluated. If the ΔV associated to the partial branch exceeds a given threshold the whole branch is

⁵ <http://adams.dm.unipi.it/gronchi/HOMEPAGE/research.html>.

discarded. This simple approach has guaranteed convergence to the global optimum for a given allowable ΔV_{max} budget and is very fast. The major limitation is represented by the required memory storage if the upper limit on the ΔV budget is increased. In this case the length of the sequence also increases but the total volume of possible alternative sequences grows considerably. Future work will be devoted to have an adaptive adjustment of the threshold to allow a better exploration while limiting the excessive use of memory. A graphical representation of the binary tree and of its working mechanism is given in Figs. 3 and 4.

After this process, for each value of M_0 on the initial orbit, the vector \mathbf{b} is translated into a list of N asteroids $\mathcal{A} = \{A_1, A_2, A_3, \dots, A_N\}$, with $N \leq n$ and $\Delta V \leq \Delta V_{max}$. The initial orbit of the spacecraft is defined by means of its orbital elements: $\mathcal{OE} = \{a, e, i, \Omega, \omega, M_0, t_0\}$, where Ω is the right ascension of the ascending node, ω is the argument of perihelion and M_0 is the mean anomaly at time t_0 . The dates of the encounters are defined as $\mathcal{T} = \{T_1, T_2, \dots, T_N\}$.

2.3. Optimisation of the sequence of asteroids

The solution found at the previous step assumes that the encounters with the asteroids take place when they are at their critical true anomalies, θ_{ast}^{MOID} , starting from an initial orbit identified by \mathcal{OE} . A better solution might however exist and could be found by changing some of the parameters of the initial orbit \mathcal{OE} (the initial mean anomaly M_0 , the semimajor and eccentricity a and e and the argument of perigee ω) or by changing the dates of encounters with the asteroids \mathcal{T} , that is by encountering the asteroids not exactly at θ_{ast}^{MOID} . In order to find a better solution, a continuous global optimisation problem is solved, in which the objective is the minimisation of the total ΔV . The upper and lower boundaries for the global optimisation problem are defined by the vectors **LB** and **UB**:

$$\mathbf{LB} = [M_0 - \Delta M_0, a - \Delta a, e - \Delta e, \omega - \Delta \omega, T_1 - \Delta T_1, \\ T_2 - \Delta T_2, \dots, T_n - \Delta T_n]^T \quad (2)$$

$$\mathbf{UB} = [M_0 + \Delta M_0, a + \Delta a, e + \Delta e, \omega + \Delta \omega, T_1 + \Delta T_1, \\ T_2 + \Delta T_2, \dots, T_n + \Delta T_n]^T \quad (3)$$

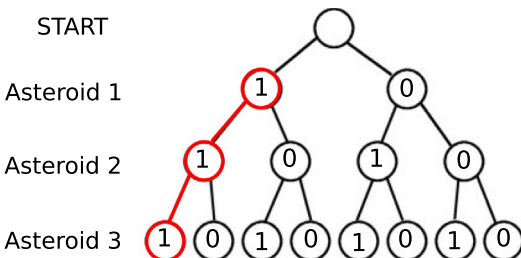


Fig. 3. Representation of the binary tree. Branches with ΔV higher than threshold (example, in red in the figure) are discarded. (For interpretation of the references to colour in this figure legend, the reader is referred to the web version of this article.)

The global search is realised using the global optimiser Multi Population Adaptive Inflationary Differential Evolution Algorithm (MP-AIDEA) (Di Carlo et al., 2015). MP-AIDEA is a multi-population adaptive version of Inflationary Differential Evolution which combines Differential Evolution (DE) (Price et al., 2006) with the working principles of Monotonic Basin Hopping Algorithm (MBH) (Wales and Doye, 1997) (see Vasile et al. (2011)). MP-AIDEA has been extensively tested on various benchmarks of difficult problems and was shown to be very effective at solving complex trajectory optimisation problems compared to other state-of-the-art global optimisation methods.

2.4. Transfer from Earth to the main belt

This section describes the transfer strategy from the Earth to the first orbit in the main belt, $\mathcal{OE} = \{a, e, i, \Omega, \omega, M_0, t_0\}$. The transfer is realised by injecting the spacecraft into an intermediate phasing orbit, characterised by orbital elements $\mathcal{OE}_{int} = \{a_{int}, e_{int}, i, \Omega, \omega, 0, T_L\}$ and orbital period T_{int} . T_L is the date of the launch of the spacecraft and the corresponding mean anomaly is zero because, at launch, the spacecraft is at the perihelion of the orbit (Earth). The ΔV required for the launch, ΔV_L , is computed as:

$$\Delta V_L = \sqrt{2 \frac{\mu_\odot}{r_\oplus} - \frac{\mu_\odot}{a_{int}}} - \sqrt{\frac{\mu_\odot}{r_\oplus}} \quad (4)$$

where μ_\odot is the Sun's planetary constant and r_\oplus is the Sun-Earth distance. The spacecraft remains on the intermediate phasing orbit for an integer number n_{rev} of revolutions. After n_{rev} revolutions, when the spacecraft is at the perihelion r_\oplus of the intermediate phasing orbit, ΔV_M is applied to reach the final orbit of semimajor axis a :

$$\Delta V_M = \sqrt{2 \frac{\mu_\odot}{r_\oplus} - \frac{\mu_\odot}{a}} - \sqrt{2 \frac{\mu_\odot}{r_\oplus} - \frac{\mu_\odot}{a_{int}}} \quad (5)$$

The spacecraft moves then for a time:

$$\Delta T = \frac{M_0 - M_p}{n} \quad (6)$$

on the orbit \mathcal{OE} . In the previous equation M_0 is the mean anomaly on the first orbit in the main belt at t_0 , $M_p = 0$ deg is the mean anomaly at perihelion and n is the mean motion of the orbit \mathcal{OE} . For every value of n_{rev} , T_{int} has to be such that at the computed time of the launch, T_L :

$$T_L = t_0 - \Delta T - n_{rev} T_{int} \quad (7)$$

the Earth is at the perihelion of \mathcal{OE} . This allows one to identify the value of T_{int} , and, therefore, the intermediate phasing orbit \mathcal{OE}_{int} , for every \mathcal{OE} and n_{rev} .

The method described above provides an impulsive solution for the transfer from Earth to \mathcal{OE} based on the assumption that the spacecraft is injected by the launcher or an upper stage into \mathcal{OE}_{int} . When the actual launch capabilities are considered the ΔV required to inject the space-

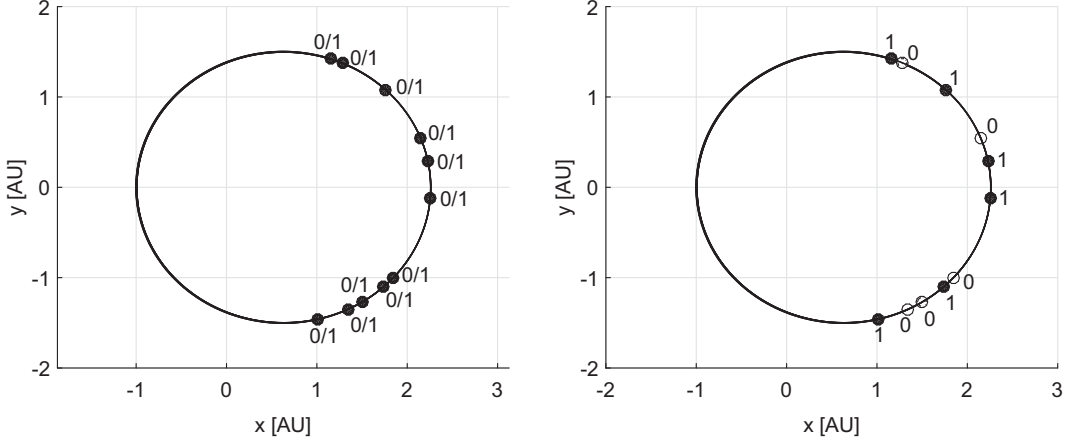


Fig. 4. Identification of the sequence of asteroids to visit using the binary tree. Each asteroid in the sequence can be assigned a value equal to 0 or 1 (left); only asteroids with associated value of 1 are visited (right).

craft into the orbit \mathcal{OE}_{int} , by means of an escape hyperbola characterised by $V_\infty = \Delta V_L$, is the sum of two contributions:

$$\Delta V_{total} = \Delta V_i(i_{inj}, \omega_{inj}) + \Delta V_{inj}(i_{inj}, \omega_{inj}) \quad (8)$$

where $\Delta V_i(i_{inj}, \omega_{inj})$ and $\Delta V_{inj}(i_{inj}, \omega_{inj})$ are, respectively, the ΔV required to change inclination from the orbit where the launcher is injecting the spacecraft to the escape hyperbola and the ΔV required to reach the required escape velocity. These ΔV 's are a function of i_{inj} and ω_{inj} , the inclination and argument of the pericentre of the escape hyperbola. The calculation of these two ΔV 's follows the approach presented in Di Carlo et al. (2017b). No consideration is done about the right ascension of the asymptote because any required right ascension of departure may be achieved by changing the time of day at which the spacecraft is launched (Kemble, 2006). Once ΔV_{total} has been found, the dry and propellant masses of the upper stage, $m_{dry}^{U/S}$ and $m_{prop}^{U/S}$, can be found from:

$$\frac{m_{prop}^{U/S}}{m_{prop}^{U/S} + m_{dry}^{U/S}} = k \quad (9)$$

$$m_0 + m_{dry}^{U/S} = \left(m_{dry}^{U/S} + m_{prop}^{U/S} + m_0 \right) \exp \left(-\frac{\Delta V_{total}}{I_{sp}^{U/S} g_0} \right)$$

where k and $I_{sp}^{U/S}$ are the propellant mass fraction and specific impulse of the upper stage and m_0 is the initial wet mass of the low-thrust spacecraft. In this paper it is assumed that the launcher injects the spacecraft in a Geostationary-Transfer Orbit (GTO). The total payload mass that the launcher has to inject into GTO is, therefore, $m_{pl} = m_0 + m_{prop}^{U/S} + m_{dry}^{U/S}$.

2.5. Low-thrust optimisation

The outcome of the sequence finder and optimisation with MP-AIDEA is a sequence of transfer legs charac-

terised by a departure heliocentric position, an end heliocentric position, a transfer time and a departure ΔV . The low-thrust optimisation process determines, for each transfer leg, an optimal control history, for the low-thrust engine, to depart from one asteroid and reach the following asteroid in the sequence at a given time. The same process is applied also to optimise the transfer from Earth to \mathcal{OE} . In this study, a variant of the direct analytical multiple shooting algorithm proposed by Zuiani et al. (2012) and implemented in the software code FABLE (FAst Boundary-value Low-thrust Estimator) is used. More information about FABLE can be found in Di Carlo et al. (2017a). The transfer leg is split into a predefined sequence of n_{LT} finite coast and thrust arcs. Each s th arc is represented by a vector of equinoctial parameters $\mathbf{E}_s = [a_s, P_{1,s}, P_{2,s}, Q_{1,s}, Q_{2,s}, L_s]^T$, plus, in case of thrust arc, the low-thrust acceleration components, a_r , a_t and a_h expressed in a local radial-transversal reference frame as (Zuiani et al., 2012):

$$\mathbf{a}_{LT,s} = \begin{Bmatrix} a_r \\ a_t \\ a_h \end{Bmatrix}_s = \begin{Bmatrix} \epsilon_s \cos \alpha_s \cos \beta_s \\ \epsilon_s \sin \alpha_s \cos \beta_s \\ \epsilon_s \sin \beta_s \end{Bmatrix} \quad (10)$$

where α_s , β_s and ϵ_s are, respectively, the azimuth, elevation and modulus of the acceleration and $\epsilon_s = F/m_s$ is the ratio between the thrust F and the current mass of the spacecraft m_s . The mass of the spacecraft is conservatively kept constant over each transfer arc and updated at the end of the transfer according to the propellant mass spent to realise that transfer. In the following the initial mass of the spacecraft at launch m_0 will be set to a predefined value of 1000 kg. Note, however, that this assumption does not limit the validity of the results as any other initial mass at launch m'_0 can be used, provided that the thrust magnitude is scaled by the ratio m'_0/m_0 . The trajectory is analytically propagated forward from the departure point and backward from the end point (Fig. 5). The motion is

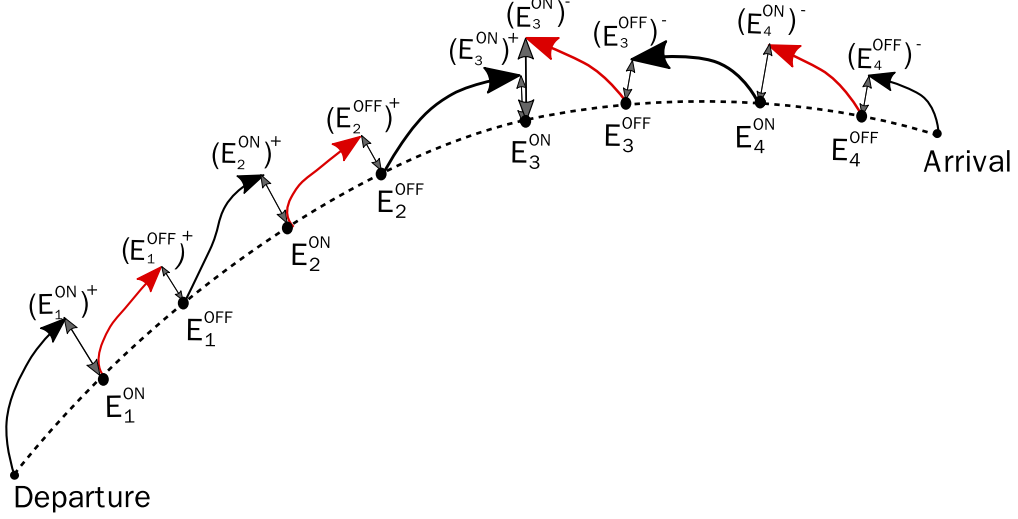


Fig. 5. Segmentation of the trajectory into coast arcs (black) and thrust arcs (red). Each node is identified by a vector of equinoctial parameters, \mathbf{E}_s . In particular, \mathbf{E}_s^{ON} nodes define the switching point from a coast to a thrust arc while \mathbf{E}_s^{OFF} nodes define the switching point from a thrust to a coast arc. (For interpretation of the references to colour in this figure legend, the reader is referred to the web version of this article.)

assumed purely Keplerian along coast arcs while thrust arcs are analytical propagated using the asymptotic expansion solutions proposed in the work of [Zuiani and Vasile \(2015\)](#). Each arc begins and ends at an On/Off control node, where On nodes define the switching point from a coast to a thrust arc and Off nodes define the switching point from a thrust to a coast arc (see Fig. 5). Therefore, thrust arcs are defined by a set of orbital elements at an On node, E_s^{ON} , and coast arcs are defined by a set of orbital elements at an Off node, E_s^{OFF} . The approach implemented in FABLE was shown to provide fast convergence to nearly optimal solutions. For more information the interested reader can refer to [Zuiani et al. \(2012\)](#) and [Zuiani and Vasile \(2015\)](#). For the trajectories considered in this study, the angle β is set to zero, since the transfers are all on the ecliptic plane and require no change of inclination (Section 3 and 4). This is a consequence of the assumptions and methods described in Section 2: the fly-bys of the asteroids take place at the MOID points of the spacecraft's heliocentric elliptic orbit and asteroids' orbits. The azimuth angles α_s are, instead, optimisation variables. The optimisable vector for each transfer is, therefore, defined by the azimuth angles α_s , for each thrust arc, and the equinoctial elements at each On and Off point:

$$\mathbf{x}_{LT} = [\alpha_1, \mathbf{E}_1^{ON}, \mathbf{E}_1^{OFF}, \alpha_2, \mathbf{E}_2^{ON}, \mathbf{E}_2^{OFF}, \dots, \alpha_{n_{LT}}, \mathbf{E}_{n_{LT}}^{ON}, \mathbf{E}_{n_{LT}}^{OFF}]^T \quad (11)$$

The optimisation problem is formulated as the following non-linear programming problem whose objective is the total ΔV for each transfer:

$$\min_{\mathbf{x}_{LT}} \Delta V = \sum_s \epsilon_s \Delta t_s(\mathbf{x}_{LT}), \quad (12)$$

where $\Delta t_s(\mathbf{x}_{LT})$ is the time length of each thrust arc, subject to the following constraints:

$$\left\{ \begin{array}{ll} (\mathbf{E}_1^{ON})^+ = \mathbf{E}_1^{ON} & \\ (\mathbf{E}_s^{OFF})^+ = \mathbf{E}_s^{OFF} & s = 1, \dots, n_{LT}/2 \\ (\mathbf{E}_s^{ON})^- = \mathbf{E}_s^{ON} & s = n_{LT}/2 + 1, \dots, n_{LT} \\ (\mathbf{E}_{n_{LT}/2+1}^{ON})^+ = (\mathbf{E}_{n_{LT}/2+1}^{ON})^- & \\ (\mathbf{E}_{n_{LT}}^{OFF})^- = \mathbf{E}_{n_{LT}}^{OFF} & \\ \sum_{s=1}^{n_{LT}} \Delta t_s = ToF & \end{array} \right. \quad (13)$$

The plus and minus signs in the constraints equations indicate, respectively, the forward integration arc and the backward integration arc. The non-linear programming problem is solved using the Matlab®*fmincon-interior-point* algorithm.

3. Results Database 1

The first search for optimal tours considers the asteroids in the database of scientific interesting asteroids (Database 1). This section presents the results of the scan of all possible sequences, with estimated cost lower than $\Delta V_{max} = 1$ km/s, and the low-thrust optimisation of the most promising solution.

3.1. Minimum orbit intersection distance

The MOID is computed between all the asteroids in the database and different orbits of the spacecraft identified by

Table 1

Orbital elements of the different possible initial orbits of the spacecraft used for the computation of the MOID with the asteroids of Database 1.

r_p [AU]	r_a [AU]	i [deg]	Ω [deg]	ω [deg]
1	[1.8, 4]	[0, 30]	0	[0, 360]

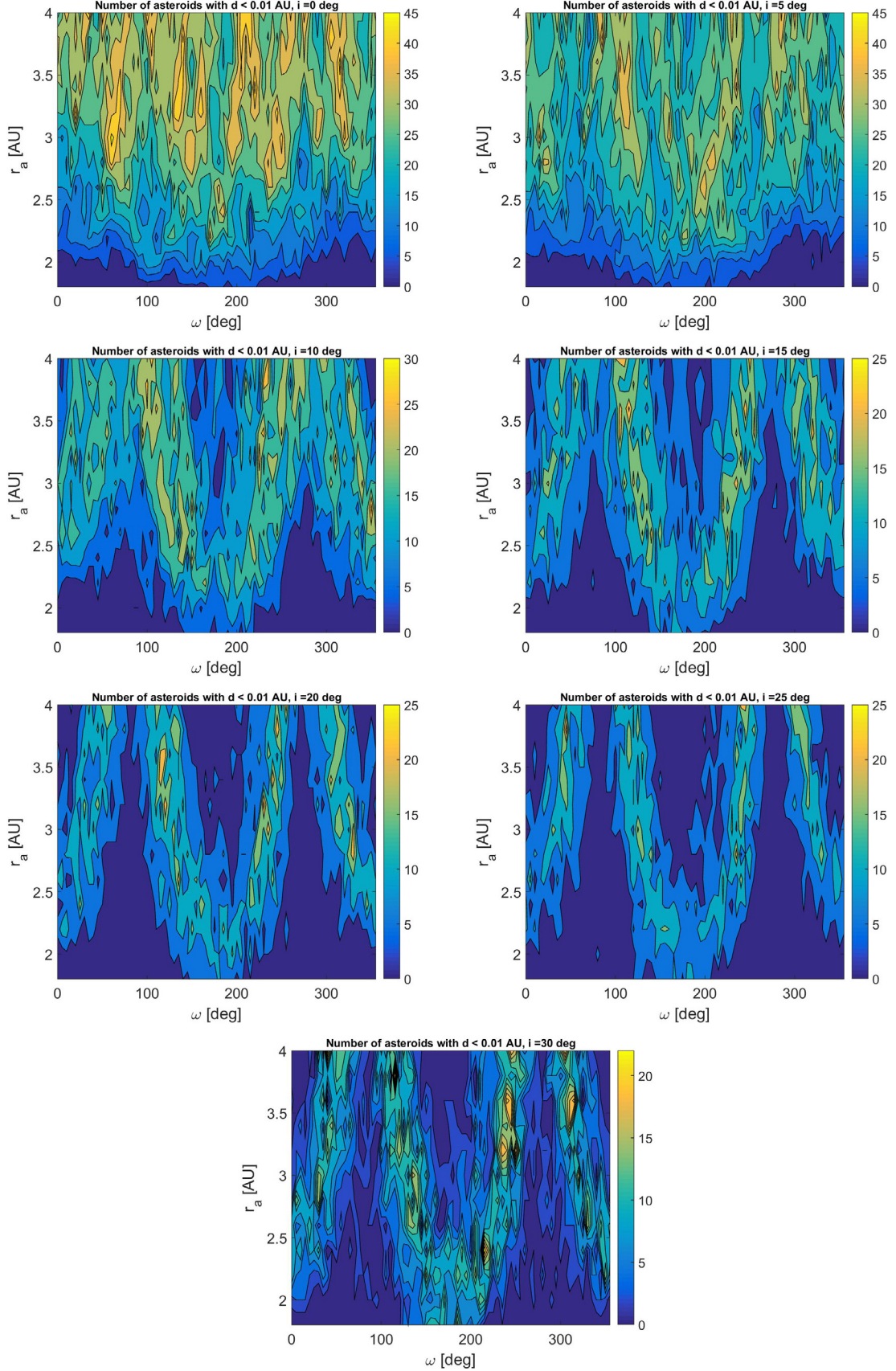


Fig. 6. Number of asteroids in Database 1 with $d < 0.01$ AU for different initial orbits of the spacecraft. The initial orbits of the spacecraft are identified by different values of r_a (y axis of each figure), ω (x axis) and i , from $i = 0$ deg (top left) to $i = 30$ deg (bottom).

the orbital elements in [Table 1](#). The spacecraft orbits are elliptical, with perihelion r_p at the Earth and aphelion r_a in a given range of distances from the Sun. [Fig. 6](#) shows, for the considered values of r_a , ω and i , the number of asteroids with $d < 0.01$ AU with respect to the orbit of the spacecraft. Results show that this number increases with decreasing inclination. As the inclination increases a dependence on the argument of the perihelion of the orbit become also evident and large regions where the number of asteroids with $d < 0.01$ AU is zero appear.

The number of asteroids shown in [Fig. 6](#) does not account for the position of asteroids and spacecraft on their orbits. Once the phasing process presented in [Section 2.1](#) is applied, the number of possible asteroids to encounter with $d < 0.01$ is further reduced. In particular, after phasing, two orbits characterised by the highest number of encounters with the asteroids in Database 1 can be identified. The orbital elements of these two orbits (O1 and O2) are given in [Table 2](#).

The number of possible encounters for different values of M_0 from 0 to 359 deg, for the orbits defined in [Table 2](#), is shown in [Fig. 7](#). Results show that the maximum number of asteroids that it is possible to visit in 5 years is 8. The cost associated to the mission has however to be computed to verify that it is below the limit value of $\Delta V_{max} = 1$ km/s.

3.2. Study of the possible sequence of asteroids

[Figs. 8 and 9](#) show the ΔV required for the tour of the asteroids in Database 1, as a function of the number N of objects visited, for the two orbits defined in [Table 2](#)

Table 2

Orbits providing the higher number of encounters with asteroids in Database 1.

	a [AU]	e	i [deg]	Ω [deg]	ω [deg]
O1	2.2	0.5455	0	0	220
O2	2.3	0.5652	0	0	315

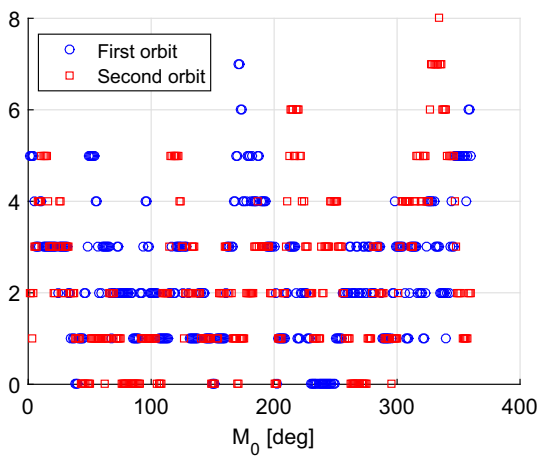


[Fig. 7](#). Number of asteroids with $d < 0.01$ and phasing condition ([Eq. 1](#)) satisfied.

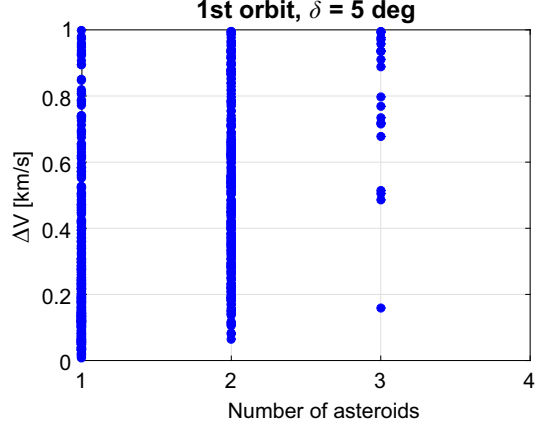


[Fig. 8](#). Relation between ΔV and number of visited asteroids for the orbit O1 for $\Delta V_{max} = 1$ km/s.

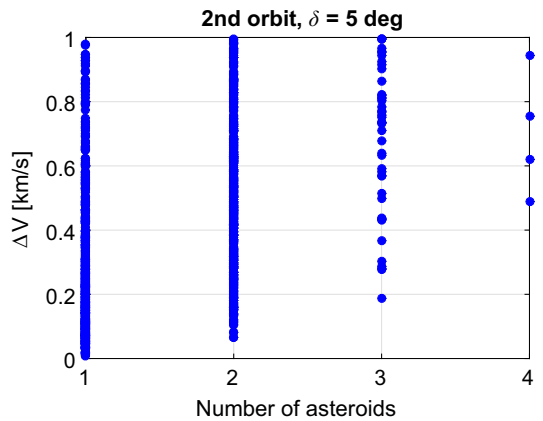


[Fig. 9](#). Relation between ΔV and number of visited asteroids for the orbit O2 for $\Delta V_{max} = 1$ km/s.

Table 3

Sensitivity of the number of solutions to δ .

δ [deg]	O1		O2	
	N_{TOT}	N_3	N_{TOT}	N_4
5	1058	20	1532	4
1	528	4	700	0
0.5	324	2	428	0
0.25	172	1	198	0

Table 4

Parameters for the definition of **UB** and **LB**.

ΔM_0 [deg]	Δa	Δe	$\Delta \omega$	ΔT_i [days]
1	0.01 a	0.01 e	0.01 ω	10

Table 5

Optimisation of the ΔV of the longest sequence of asteroids for the two orbits defined in [Table 2](#).

Orbit	N	δ [deg]	ΔV [km/s]	ΔV_{opt} [km/s]
O1	3	5	0.1580	0.1024
O2	4	5	0.4881	0.3057

Table 6

Selected solution for the main belt tour for Database 1.

Targeted asteroid	Dep. date	Optimised dep. date	ToF [days]	Opt. ToF [days]	ΔV [m/s]	Opt. ΔV [m/s]
2006 UJ47	01/01/2030	01/01/2030	294.25	294.02	80.34	67.58
2007 UV	22/10/2030	22/10/2030	363.64	364.22	147.52	105.63
2005 YN176	20/10/2031	21/10/2031	207.00	206.78	137.87	132.44
Ockeghem	14/05/2032	15/05/2032	694.30	689.37	122.39	0.0004
					488.12	305.67

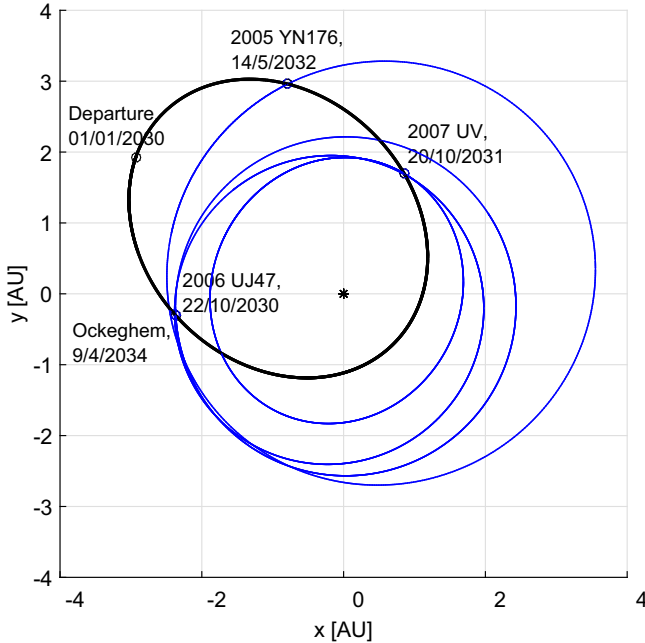


Fig. 10. Trajectories of the selected solution for the main belt tour for Database 1.

and $\Delta V_{max} = 1$ km/s. The figures collect the results obtained for all the possible values of M_0 from 0 to 359 deg, at steps of 1 deg. Results show that, within the limit of $\Delta V_{max} = 1$ km/s, the maximum number of asteroids that is possible to visit is $N = 3$ for O1 and $N = 4$ for O2. The total computation time to obtain these results, for all the values of M_0 ranging from 1 to 359 deg, is 1 s on a Intel (R) Core(TM) i7-3770 CPU 3.4 GHz and 8 GB RAM using Matlab R2015a. The length n of the binary vector \mathbf{b} ranges from 1 to 7, depending on M_0 .

Results in Figs. 8 and 9 are obtained using $\delta = 5$ deg. The sensitivity of the results on the value of δ is presented in Table 3, where the total number of solutions N_{TOT} and the number of solutions with 3 or 4 visited asteroids, N_3 and N_4 , are presented for different values of δ . Results show that the total number of solutions N_{TOT} and the number of solutions with 3 or 4 visited asteroids decrease with δ .

3.3. Optimisation of the sequence of asteroids

The best solutions in Figs. 8 and 9 are optimised with MP-AIDEA. The lower and upper boundaries **LB** and **UB** used for the optimisation with MP-AIDEA are defined

by Eqs. (2) and (3) and the values reported in Table 4. The intervals Δa , Δe and $\Delta \omega$ are given as a function of the nominal values, a , e and ω . MP-AIDEA is run for 50,000 function evaluations and the optimisation is repeated 25 times. The best solution obtained at the end of this process is then considered.

Table 5 shows the best optimised ΔV_{opt} , together with the number of visited asteroids N , the angle δ and the initial ΔV before the optimisation with MP-AIDEA.

The solution selected for the low-thrust optimisation is the one associated to orbit 2 (O2) in Table 2, as it allows to encounter 4 rather than 3 asteroids of Database 1. Details of the transfer are given in Table 6 and in Fig. 10. The initial orbit in the main belt is characterised by orbital elements: $\mathcal{OE}_1 = \{a = 2.2945 \text{ AU}, e = 0.5652, i = 0 \text{ deg}, \Omega = 0 \text{ deg}, \omega = 315.2038 \text{ deg}, M_0 = 214.8032 \text{ deg}, t_0 = 10958.5 \text{ MJD2000}\}$ Asteroid 2006 UJ47 is a fast rotator, characterised by a rotation period of 0.64 h. The other three asteroids in Table 6 are asteroid pairs. Asteroid pairs are defined as asteroids that had a very small relative velocity at some point in the past, in the order of m/s.⁶ They may represent former binary asteroids or the result of collisional breakup of a parent asteroid.

3.4. Transfer from Earth to the main belt

The tour in Table 6 satisfies the 5 year requirement. The attempt now is to realise the launch and transfer to orbit \mathcal{OE}_1 in less than 5 years so that the mission time is less than 10 years. Two possibilities exist for the transfer from the Earth to the selected orbit \mathcal{OE}_1 , with time of transfer shorter than 5 years. The details of these options are given in Table 7 and the orbits are shown in Figs. 11 and 12. In Table 7 the times T_L and T_M when ΔV_L and ΔV_M are applied, the corresponding ΔV and the orbital elements of the intermediate phasing orbit are given.

The launch for the two options T1 and T2 defined in Table 7 is investigated for two types of launchers: the Indian Space Research Organisation GSLV-D6 (Geosynchronous Satellite Launch Vehicle)⁷ and the European Space Agency Soyuz.⁸ The GTO parameters of the GSLV and Soyuz launchers are summarised in Table 8, together

⁶ <http://www.johnstonsarchive.net/astro/asteroidpairs.html>.

⁷ Indian Space Research Organisation – <http://www.isro.gov.in/launcher/gslv-d6>.

⁸ Arianespace – <http://www.arianespace.com/vehicle/soyuz/>.

Table 7

Transfers to the orbit characterised by orbital elements \mathcal{OE}_1 with transfer time shorter than 5 years.

T_L	ΔV_L [km/s]	a_{int} [AU]	e_{int}	n_{rev}	T_M	ΔV_M [km/s]	ΔT [days]	
T1	06/08/2026	2.4879	1.2107	0.1740	1	05/12/2027	4.9785	757.44
T2	06/08/2025	5.8463	1.7577	0.4311	1	05/12/2027	1.6202	757.44

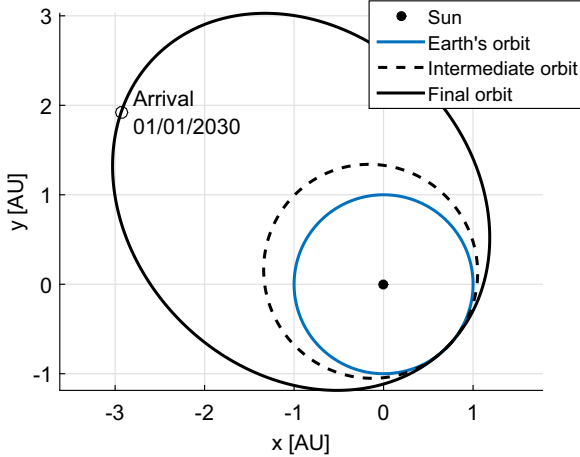
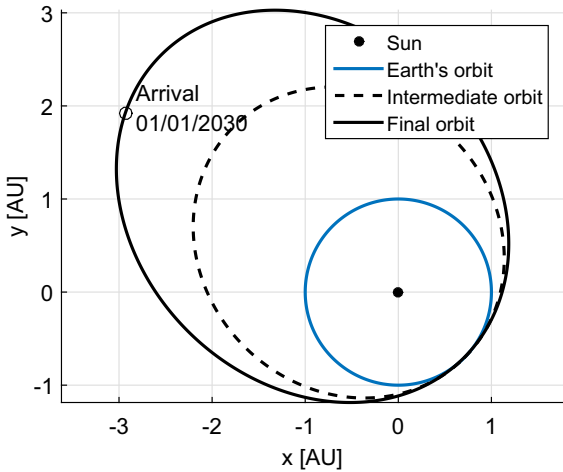
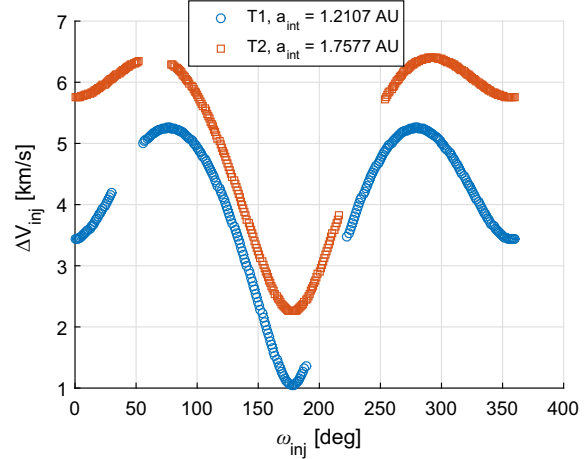
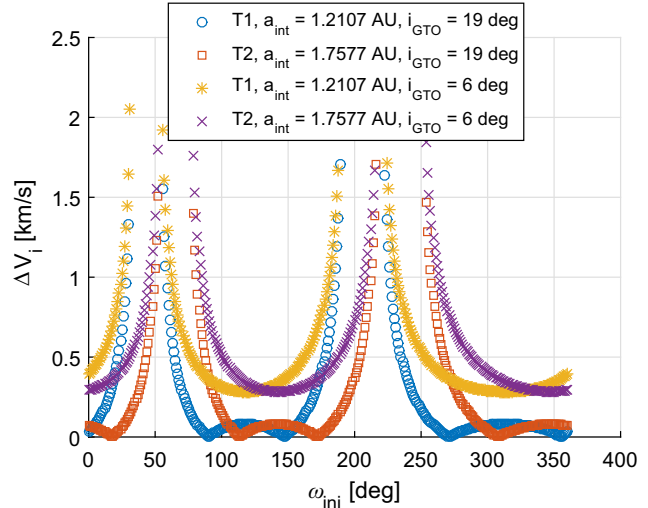
Fig. 11. Transfer T1 to the orbit characterised by orbital elements \mathcal{OE}_1 .Fig. 12. Transfer T2 to the orbit characterised by orbital elements \mathcal{OE}_1 .Fig. 13. Variation of ΔV_{inj} with the argument of perigee of the hyperbolic orbit for the two transfer options to \mathcal{OE}_1 .Fig. 14. Variation of ΔV_i with the argument of perigee of the hyperbolic orbit for the transfer options to \mathcal{OE}_1 and the two launchers considered.

Table 8

Orbital elements and payload mass in GTO: GLSV and Soyuz.

	$h_{p,GTO}$ [km]	$h_{a,GTO}$ [km]	i_{GTO} [deg]	ω_{GTO} [deg]	m_{GTO} [kg]
GLSV	170	35,975	19	178	2330
Soyuz	250	35,943	6	178	3250

with their maximum payload mass in GTO, m_{GTO} . The quantities $h_{p,GTO}$ and $h_{a,GTO}$ are the perigee altitude and apogee altitude of the GTO orbit.

Following the method described in Section 2.4, results for the two transfer options T1 and T2 and for the two launchers are shown in Figs. 13–15.

Fig. 13 shows the ΔV necessary for the injection into the hyperbolic orbit from the GTO, ΔV_{inj} . Notice that ΔV_{inj} depends only on ω_{inj} . Fig. 14 presents the ΔV necessary for the inclination change from the inclination of the GTO to the appropriate inclination of the hyperbolic orbit. ΔV_i depends on both the considered intermediate phasing orbit (T1 or T2) and on the launcher chosen, since the GTO of GLSV and Soyuz have different inclinations. Finally, the total ΔV_{total} , given by the sum of ΔV_{inj} and ΔV_i , is presented in Fig. 15. The minimum ΔV results are summarised in Table 9, that reports the inclination and

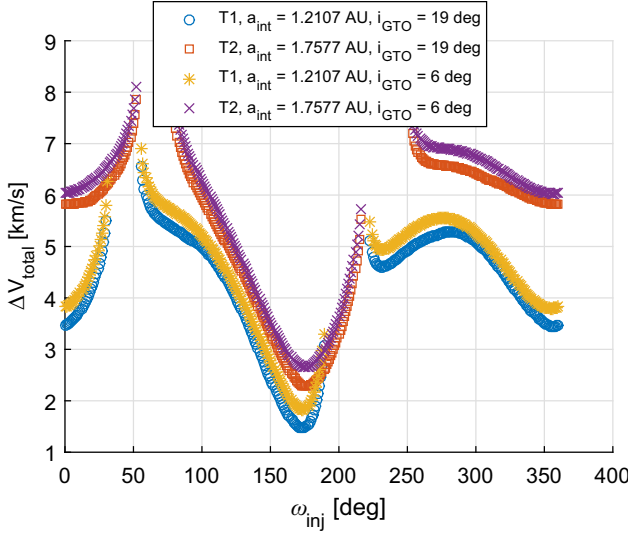


Fig. 15. Variation of $\Delta V_{total} = \Delta V_{inj} + \Delta V_i$ with the argument of perigee of the hyperbolic orbit for the two transfer options to $\mathcal{O}\mathcal{E}_1$ and the two launchers considered.

argument of perigee of the injection hyperbolic orbit, the ΔV 's, the propellant mass and dry mass of the upper stage, $m_{prop}^{U/S}$ and $m_{dry}^{U/S}$, the total payload mass in GTO, m_{pl} , and the launcher mass margin. The assumed initial wet mass of the spacecraft is $m_0 = 1000$ kg and the considered upper stage has $I_{sp}^{U/S} = 400$ s and propellant mass fraction $k = 0.77$. Results show that, for this mass of the spacecraft, the injection into T1 could be realised using GLSV, while for T2 a Soyuz launch would be required. It is worth to recall that the reference value of m_0 chosen in this study can be changed without the need to redesign the tour and the transfer provided that the thrust is rescaled accordingly (Section 3.5). The mass margins shown in Table 9 give indication about the values of m_0 that is possible to consider for each launch option and each launcher. For example, option T1, using Soyuz, would allow to increase the mass of the spacecraft, since the mass margin is 1311.04 kg. On

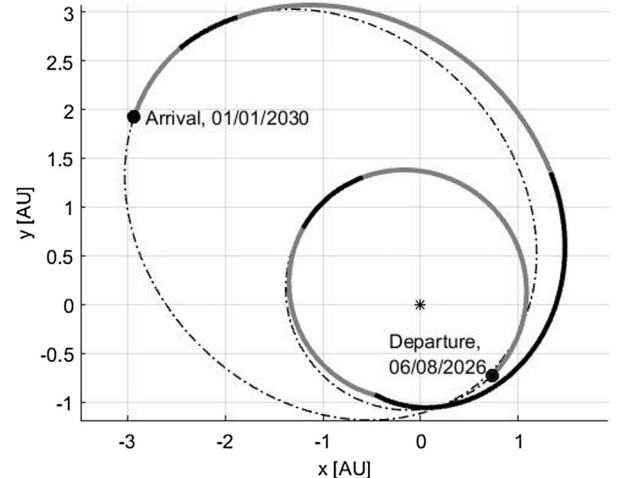


Fig. 16. Low-thrust transfer trajectory to $\mathcal{O}\mathcal{E}_1$, option T1.

the contrary, a launch with option T2 and GLSV would require a smaller spacecraft than the proposed 1000 kg.

3.5. Low-thrust optimisation

The electric engine considered in this study has thrust magnitude $F = 0.15$ N and specific impulse $I_{sp} = 3000$ s. The initial mass of the spacecraft at launch is assumed to be $m_0 = 1000$ kg. This corresponds to a low-thrust acceleration equal to $1.5 \cdot 10^{-4}$ m/s². Results for different initial mass of the spacecraft can be obtained by scaling the results presented here, under the assumption that the thrust level increases with the mass of the spacecraft, so that the acceleration is always $1.5 \cdot 10^{-4}$ m/s². The low-thrust ΔV required to realise the transfer to $\mathcal{O}\mathcal{E}_1$ and the tour of the asteroids is shown in Table 10, together with the propellant consumption m_{prop} and the initial and final masses, m_0 and m_f , for the two phases of the mission (transfer to $\mathcal{O}\mathcal{E}_1$ and tour of the asteroids). Both the possible transfer options defined in Table 7 are considered. The low-thrust trajectories for the transfer phase T1 and T2 are shown in Figs. 16

Table 9
Launch and injection into intermediate phasing orbit (Database 1).

	i_{inj} [deg]	ω_{inj} [deg]	ΔV_i [km/s]	ΔV_{inj} [km/s]	ΔV_{total} [km/s]	m_{dry}^{US} [kg]	m_{prop}^{US} [kg]	m_{pl} [kg]	Margin [kg]
T1, GLSV	31.42	173	0.34	1.12	1.47	156.89	525.26	1682.16	647.84
T2, GLSV	19.89	176	0.02	2.26	2.28	308.46	1032.67	2341.14	-11.14
T1, Soyuz	31.28	173	0.70	1.13	1.83	215.96	722.99	1938.96	1311.04
T2, Soyuz	19.84	176	0.38	2.27	2.65	407.03	1362.66	2769.69	480.31

Table 10
 ΔV and propellant consumption for the low-thrust transfer to $\mathcal{O}\mathcal{E}_2$ and for the asteroids tour of Database 1.

	Transfer to $\mathcal{O}\mathcal{E}_1$				Asteroids tour			
	m_0 [kg]	ΔV [km/s]	m_{prop} [kg]	m_f [kg]	m_0 [kg]	ΔV [km/s]	m_{prop} [kg]	m_f [kg]
T1	1000	4.0604	129	871	871	0.8881	25.91	845.09
T2	1000	1.9582	64.43	935.57	935.57	0.7236	22.75	912.82

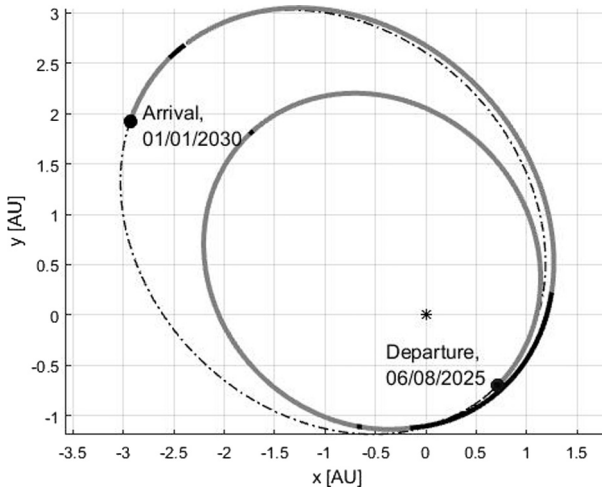
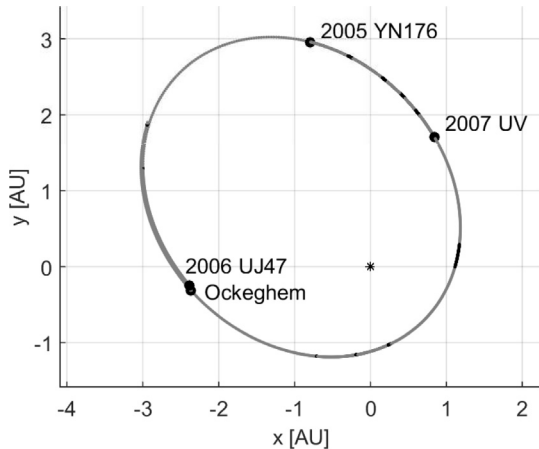
Fig. 17. Low-thrust transfer trajectory to $\mathcal{O}\mathcal{E}_1$, option T2.

Fig. 18. Low-thrust trajectory for the tour of the asteroids of Database 1.

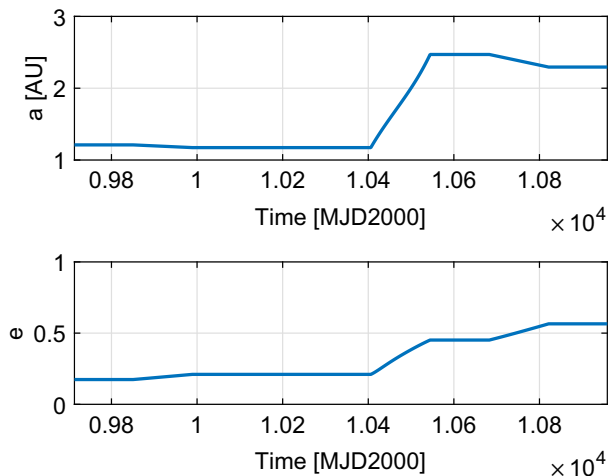
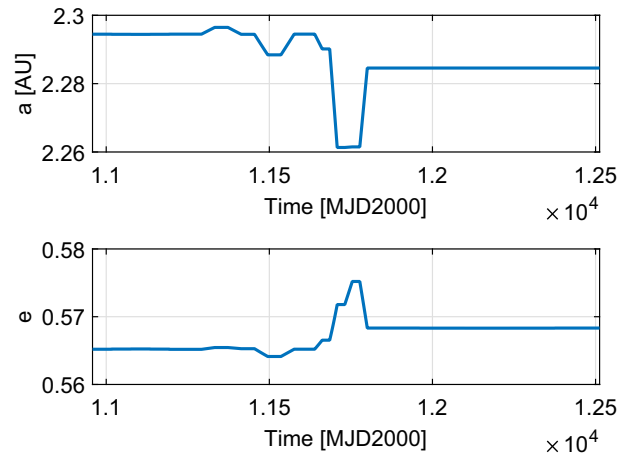
Fig. 19. Variation of semimajor axis and eccentricity during the low-thrust transfer to $\mathcal{O}\mathcal{E}_1$.

Fig. 20. Variation of semimajor axis and eccentricity during the low-thrust transfertour of the asteroids of Database 1.

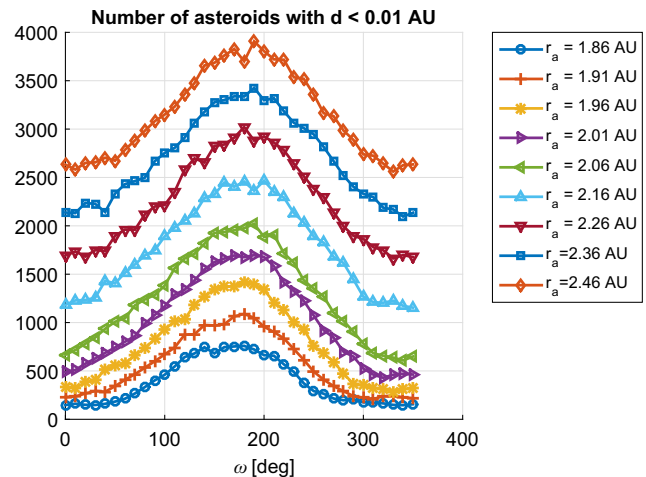
and 17, with coast arcs in gray and thrust arcs in black. The low-thrust trajectory for the tour phase corresponding to T1 is shown in Figs. 18 while Figs. 19 and 20 show the variation of a and e along the trajectory. Transfer option T2 allows for a higher final spacecraft mass (912.82 kg rather than 845.09 kg) but the transfer time is one year longer and the ΔV required for the injection into orbit is higher (Table 9).

4. Results Database 1 + 2

Results from Section 3 show that the maximum number of scientifically interesting asteroids that can be visited is four. The main belt, however, houses more than 641,933

Table 11
Orbital elements of the different possible initial orbits of the spacecraft used for the computation of the MOID.

r_p [AU]	r_a [AU]	i [deg]	Ω [deg]	ω [deg]
1	[1.86, 2.46]	0	0	[0, 360]

Fig. 21. Number of asteroids with $d < 0.01$ AU for different initial orbit of the spacecraft, identified by their aphelion radius r_a .

objects; with such a large number of objects, additional asteroids of reduced scientific interest might be visited while travelling between two asteroids in Database 1. In order to study this scenario, the two Databases 1 and 2 were combined and new sequences were generated. This section presents the results of this analysis.

4.1. Minimum orbit intersection distance

As before, the MOID is computed between all the asteroids in the combined database and different orbits of the spacecraft identified by the orbital elements in Table 11.

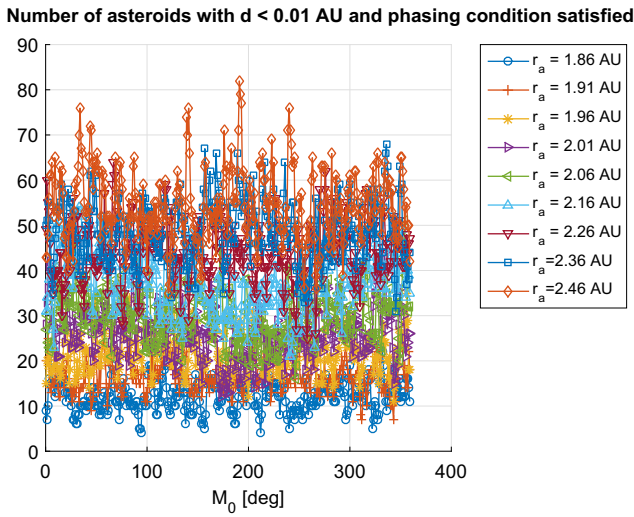


Fig. 22. Number of asteroids with $d < 0.01$ AU and phasing condition for asteroids encounter (Eq. 1) satisfied.

Fig. 21 shows, for each analysed value of the aphelion r_a and for different values of ω , the number of asteroids with $d < 0.01$ AU with respect the orbit of the spacecraft. As before, the higher the aphelion the greater the number of asteroids with $d < 0.01$ AU. This is true in the range of r_a considered in this study. We then apply the phasing process presented in Section 2.1 to further reduce the shortlist. **Fig. 22** shows the number of asteroids that respect the condition in Eq. 1, for different values of M_0 and for the value of ω giving the maximum number of asteroids with $d < 0.01$ AU; $\delta = 1$ in this case. The number of asteroids with $d < 0.01$ AU and phasing condition satisfied can be as high as 82, when $r_a = 2.46$ AU. However, only transfers with a total ΔV lower than ΔV_{max} are considered. The sequence of asteroids that satisfy $\Delta V < \Delta V_{max}$ are presented in the next section.

4.2. Study of the possible sequences of asteroids

Fig. 23 shows the ΔV required for the tour of the asteroids, as a function of the number N of visited objects. The initial orbit of the spacecraft has $r_a = 1.86$ AU and $\omega = 180$ deg and the maximum mission cost is $\Delta V_{max} = 1$ km/s. Different values of the angle δ are considered, from $\delta = 0.1$ deg to $\delta = 1$ deg. The values of δ used in this section are different from the one used in Section 3. The dimension of the considered database of asteroids ($\sim 100,000$ vs. ~ 400) results in unmanageable computational time and amount of data generated when δ is larger than the value used here. **Fig. 23** collects the results for all the possible values of M_0 from 1 to 359 deg, at steps of 1

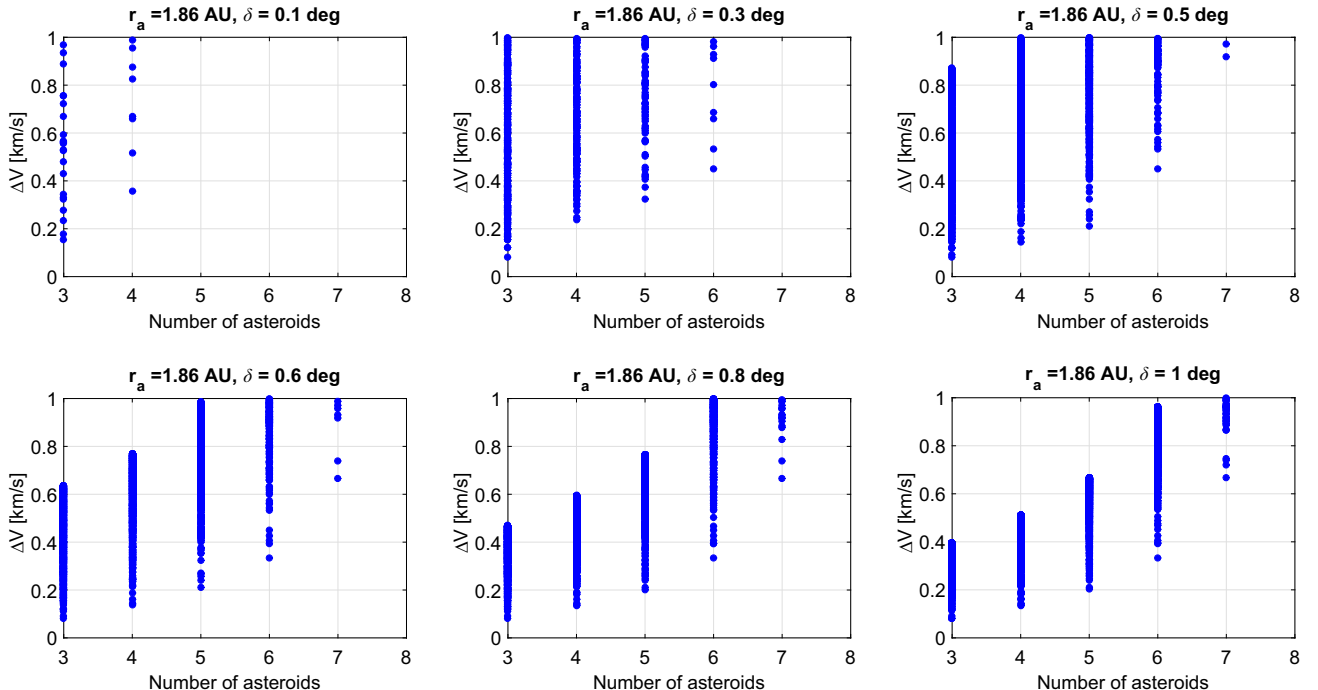


Fig. 23. Relation between ΔV and number of visited asteroids for orbit with $r_a = 1.86$ AU and different values of δ .

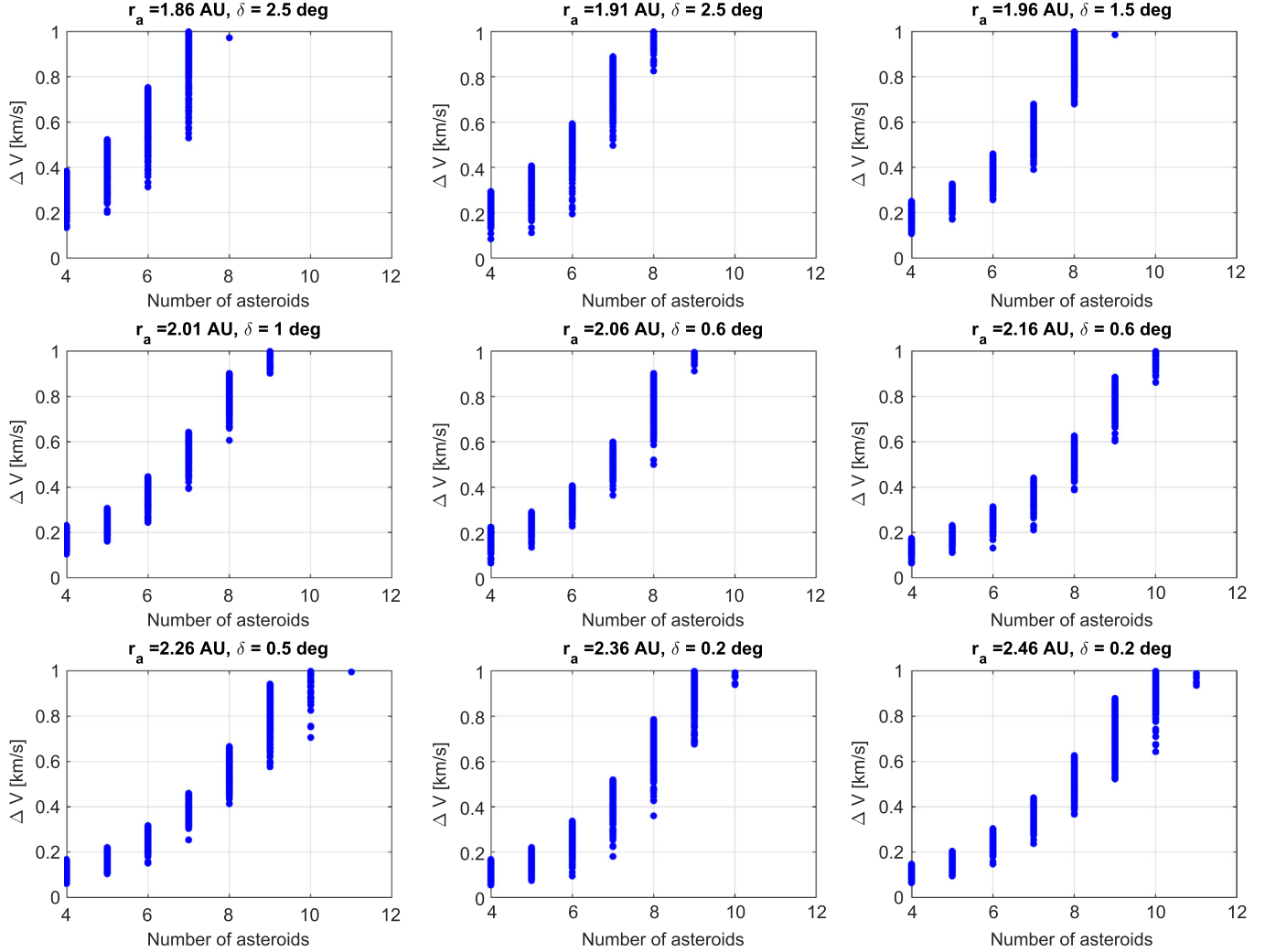


Fig. 24. Relation between ΔV and number of visited asteroids for orbits with different r_a and for different values of δ .

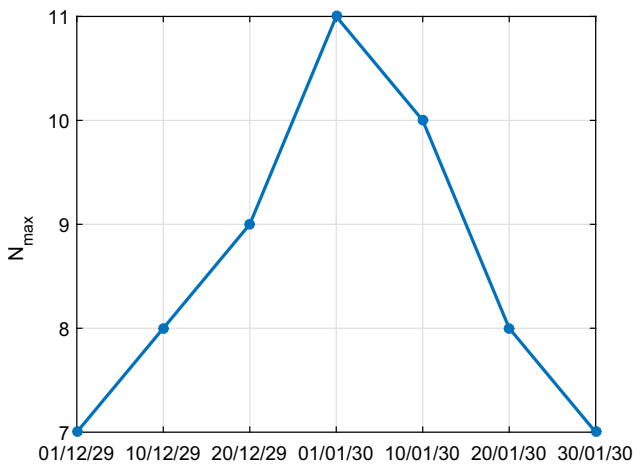


Fig. 25. Maximum number of visited asteroids for $\Delta V_{max} = 1$ km/s and different initial date for the tour (dates in dd/mm/yy).

deg and, for each value of N , only the first 1000 best solution (the ones with lower ΔV) are shown.

Results from Fig. 23 show that higher values of δ allows one to find solutions with a longer list of asteroids, while still satisfying the condition $\Delta V < \Delta V_{max}$. The maximum value of N is indeed 4 for $\delta = 0.1$ deg and $N = 7$ for $\delta = 1$ deg. Fig. 24 shows the relation between ΔV and number of visited asteroids for orbits with different values of r_a , as defined in Table 11, and different values of δ . The value of ω for each orbit is the one that allows one to visit the maximum possible number of asteroids for that r_a . As r_a increases, the maximum number of asteroids that can be visited increases from 8, for $r_a = 1.86$ AU, to 11 for $r_a = 2.46$ AU and the ΔV associated to a given number of asteroids N decreases.

Fig. 24 shows that the maximum number of visited asteroids, $N = 11$, can be obtained using an orbit with $r_a = 2.26$ AU or $r_a = 2.46$ AU. For $r_a = 2.26$ AU and $\delta = 0.5$ deg, the binary vector \mathbf{b} composed of 0's and 1's has a length depending on the value of M_0 (M_0 ranges from 1 to 359 deg). The minimum length of \mathbf{b} is $n = 4$ and the maximum length is $n = 31$. The BPA has, therefore, to handle a maximum of 2^{31} sequences (Section 2.2). The total

Table 12

Selected solution for the main belt tour for Database 1 + 2. Interesting asteroids from Database 1 are shown in bold.

Targeted asteroid	Dep. date	Optimised dep. date	ToF [days]	Opt. ToF [days]	ΔV [m/s]	Opt. ΔV [m/s]
2012 DW5	1/1/2030	1/1/2030	78.77	81.37	80.42	62.64
2005 QM95	20/3/2030	23/3/2030	148.27	145.02	240.41	16.12
2007 UJ78	16/8/2030	15/8/2030	119.12	119.92	216.58	113.86
2003 QS31	13/12/2030	13/12/2030	392.10	392.35	101.55	108.34
2001 QY152	9/1/2032	9/1/2032	105.36	105.25	51.17	37.07
2009 HL17	23/4/2032	23/4/2032	92.23	92.34	90.53	73.30
2005 SF9	24/7/2032	25/7/2032	143.38	143.43	94.41	74.04
Moore-Sitterly	15/12/2032	15/12/2032	409.26	409.08	35.33	13.92
2000 QL	28/1/2034	28/1/2034	64.72	64.88	106.24	107.09
2000 YU15	3/4/2034	3/4/2034	264.52	264.27	147.52	123.63
2000 VT44	23/12/2034	23/12/2034	59.97	59.82	22.40	31.28
					1186.55	761.28

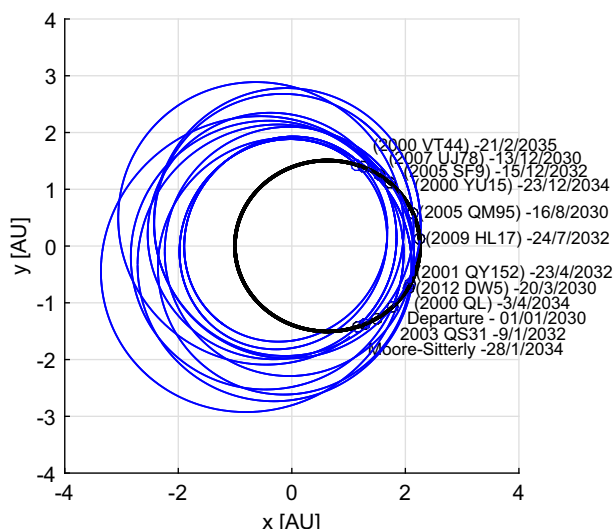


Fig. 26. Selected solution for the main belt tour for Database 1 + 2.

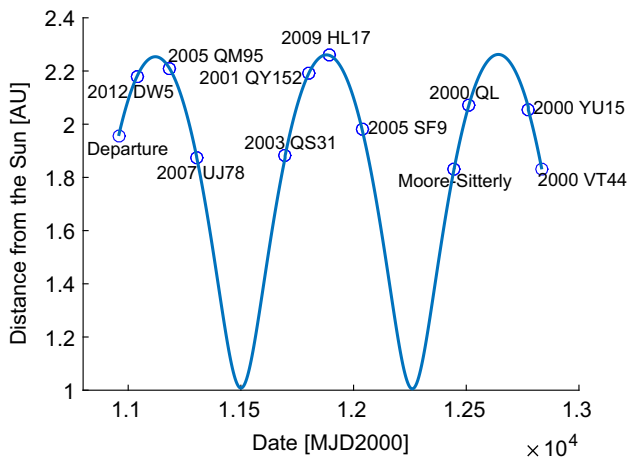


Fig. 27. Distance of the spacecraft from the Sun for the selected solution for the main belt tour for Database 1 + 2.

computation time, for all the values of M_0 ranging from 1 to 359 deg, is 82 min on a Intel(R) Core(TM) i7-3770 CPU 3.4 GHz and 8 GB RAM using Matlab R2015a. In the following the solution characterised by $r_a = 2.26$ AU is analysed in more detail. Fig. 25 shows the maximum number of asteroids that is possible to visit with maximum tour cost $\Delta V_{max} = 1$ km/s for different initial dates from December 2029 to January 2030 and $r_a = 2.26$ AU. The best results are obtained with initial date 01/01/2030, the one chosen for this study.

Since MP-AIDEA can reduce the ΔV cost of the mission, for $r_a = 2.26$ AU the binary tree for the generation of the possible sequences of asteroids is run also for $\Delta V_{max} = 2$ km/s. The aim is to obtain, after optimisation, $\Delta V_{opt} < 1$ km/s with $N \geq 11$.

Results show that, within the limit of $\Delta V_{max} = 2$ km/s, the maximum number of asteroids that can be visited is $N = 14$.

However, by inspecting all the sequences, one can see that:

- For $N = 14$, only two different sequences are identified. They do not include any of the scientifically interesting asteroids in Database 1.
- For $N = 13$, 262 possible sequences are found, none of which include asteroids from Database 1.
- For $N = 12$, 5764 sequences are found, 29 of which included 1 or 2 asteroids from Database 1. Among the 29 solutions with asteroids from Database 1, the one with lowest cost and two scientifically interesting asteroids has a $\Delta V = 1.7574$ km/s.
- For $N = 11$, 84,606 possible sequences are found, out of which 2109 include 1 or 2 asteroids from Database 1. The solution with lowest ΔV and 2 scientifically interesting asteroids has a cost of 1.1865 km/s.

Table 13

Transfers to the orbit characterised by orbital elements \mathcal{OE}_{1+2} with transfer time shorter than 5 years.

T_L	ΔV_L [km/s]	a_{int} [AU]	e_{int}	n_{rev}	T_M	ΔV_M [km/s]	ΔT [days]
T1	21/03/2028	1.5935	1.1234	0.1099	1	29/05/2029	3.6929
T2	21/03/2026	3.7491	1.3653	0.2676	2	29/05/2029	1.5374

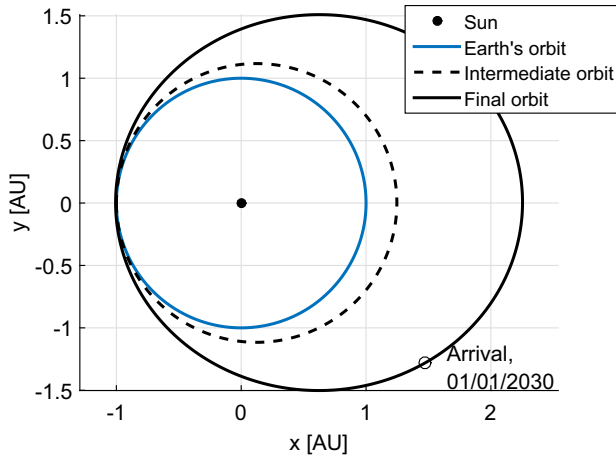


Fig. 28. Orbits for transfer option T1 from Earth to orbit $\mathcal{O}\varepsilon_{1+2}$.

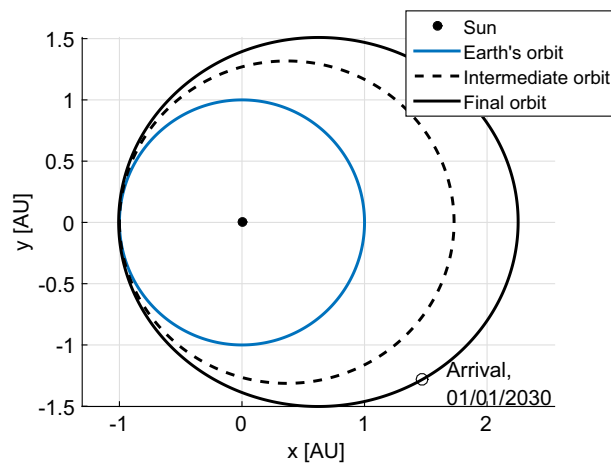


Fig. 29. Orbits for transfer option T2 from Earth to orbit $\mathcal{O}\varepsilon_{1+2}$.

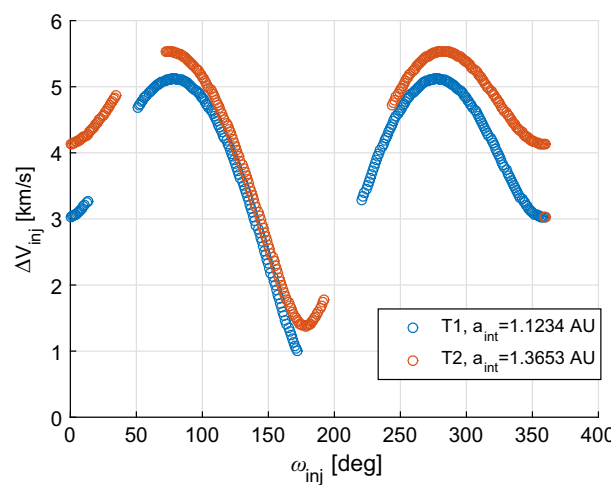


Fig. 30. Variation of ΔV_{inj} with the argument of perigee of the hyperbolic orbit for the two transfer options to $\mathcal{O}\varepsilon_{1+2}$.

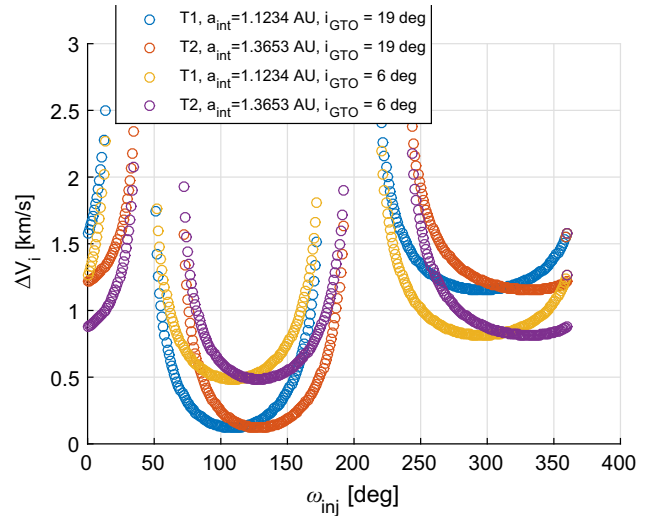


Fig. 31. Variation of ΔV_i with the argument of perigee of the hyperbolic orbit for the transfer options to $\mathcal{O}\varepsilon_{1+2}$ and the two launchers considered.

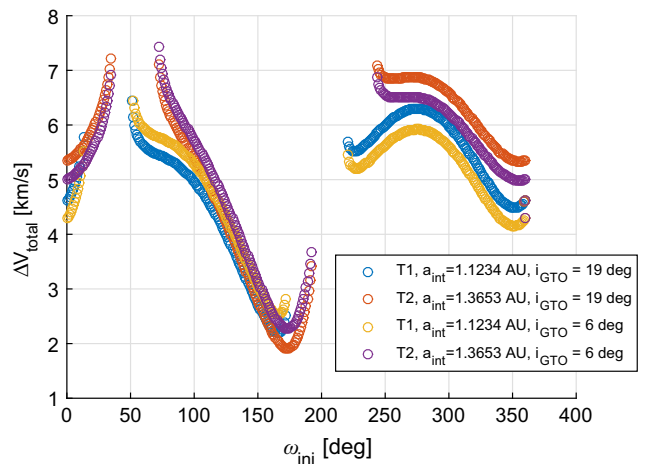


Fig. 32. Variation of $\Delta V_{total} = \Delta V_{inj} + \Delta V_i$ with the argument of perigee of the hyperbolic orbit for the two transfer options to $\mathcal{O}\varepsilon_{1+2}$ and the two launchers considered.

4.3. Optimisation of the sequence of asteroids

The solutions with $N = 11$ and $N = 12$ that include 2 asteroids from Database 1 and with lowest ΔV are further optimised using MP-AIDEA. The settings of the optimisation problem and the boundaries of the search space are the same ones used for Database 1. After optimisation, the solution characterised by $N = 12$ and $\Delta V = 1.7574$ km/s gives an optimised cost of $\Delta V_{opt} = 1.3$ km/s. The solution characterised by $N = 11$ and $\Delta V = 1.1865$ gives $\Delta V_{opt} = 0.7613$ km/s. Since in this case $\Delta V < 1$ km/s, this solution is the one selected for further analysis. Details of the asteroids visited, times of encounters and ΔV are given in Table 12, while a graphical representation is given in Figs. 26 and 27.

Table 14

Injection into intermediate phasing orbit (Database 1 + 2).

	i_{inj} [deg]	ω_{inj} [deg]	ΔV_i [km/s]	ΔV_{inj} [km/s]	ΔV_{total} [km/s]	m_{dry}^{US} [kg]	m_{prop}^{US} [kg]	m_{pl} [kg]	Margin [kg]
T1, GSLV	51.94	166	0.91	1.29	2.20	290.10	971.21	2261.31	68.69
T2, GSLV	35.93	173	0.47	1.44	1.91	230.82	772.74	2003.56	326.44
T1, Soyuz	51.73	166	1.25	1.29	2.54	374.21	1252.77	2626.98	623.02
T2, Soyuz	35.78	173	0.83	1.44	2.27	305.99	1024.42	2330.42	919.58

Table 15

 ΔV and propellant consumption for the low-thrust transfer to \mathcal{OE}_{1+2} and tour of Database 1 + 2.

	Transfer to \mathcal{OE}_{1+2}				Asteroids tour			
	m_0 [kg]	ΔV [km/s]	m_{prop} [kg]	m_f [kg]	m_0 [kg]	ΔV [km/s]	m_{prop} [kg]	m_f [kg]
T1	1000	4.1345	131.19	868.81	868.81	2.9132	81.96	786.85
T2	1000	1.4541	48.25	951.75	951.75	2.4584	76.35	875.40

The scientifically interesting asteroids are represented in bold in Table 12. Both 2003 QS31 and 2110 Moore-Sitterly are asteroid pairs.

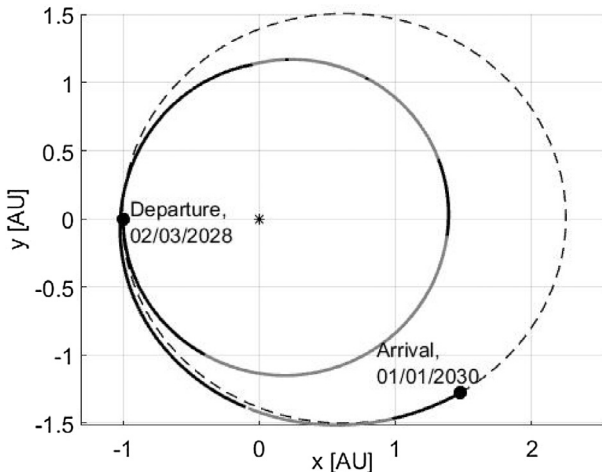
The initial orbit of the spacecraft in the main belt has optimised orbital elements: $\mathcal{OE}_{1+2} = \{a = 1.6299 \text{ AU}, e = 0.3826, i = 0 \text{ deg}, \Omega = 0 \text{ deg}, \omega = 180.3330 \text{ deg}, M_0 = 102.36 \text{ deg}, t_0 = 10958.5 \text{ MJD2000}\}$.

4.4. Transfer from Earth to the main belt

Two possibilities exist for the transfer to the orbit \mathcal{OE}_{1+2} with time of flight shorter than 5 years. These are presented in Table 13 and Figs. 28 and 29.

Following the method described in Section 2.4, results for the two transfer options T1 and T2 and for the two launchers are shown in Figs. 30–32.

The minimum ΔV results are summarised in Table 14. Both GSLV and Soyuz can be used to inject the spacecraft and upper stage into GTO, with Soyuz allowing for a larger mass margin.

Fig. 33. Low-thrust transfer trajectory to \mathcal{OE}_{1+2} , option T1.

4.5. Low-thrust optimisation

The ΔV required to realise the low-thrust transfer to \mathcal{OE}_{1+2} and the tour of the asteroids is shown in Table 15,

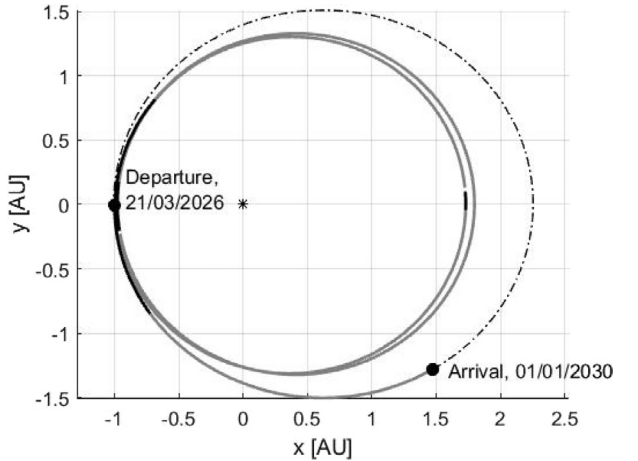
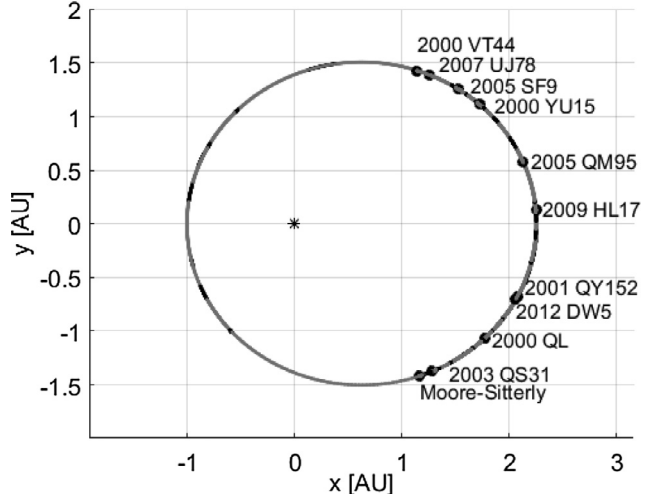
Fig. 34. Low-thrust transfer trajectory to \mathcal{OE}_{1+2} , option T2.

Fig. 35. Low-thrust trajectory for the tour of the asteroids of Database 1 + 2.

together with the propellant consumption m_{prop} and the initial and final mass, m_0 and m_f , for the two phases of the mission (transfer to \mathcal{OE}_1 and tour of the asteroids). Both the possible transfer options defined in Table 13 are evaluated.

The low-thrust trajectories for the transfer phases T1 and T2 are shown in Figs. 33 and 34. The low-thrust trajectory for the asteroid tour phase of option T1 and the corresponding variation of a and e are shown in Figs. 35–37. Table 15 shows that transfer option T2 results in a higher final mass of the spacecraft (875.40 kg) than option T1. Option T2 has also a lower ΔV_{total} than T1 (Table 14), but the transfer time is 2 years longer.

4.6. Summary of the main mission options for Database 1 and 1 + 2

The main results of the mission options for Database 1 and Database 1 + 2 are summarised in Table 16. The table gives the time of flight for the transfer from Earth to \mathcal{OE}_1 and \mathcal{OE}_{1+2} , the time of flight of the tour of the asteroids, the total ΔV to be provided by the low-thrust engine and

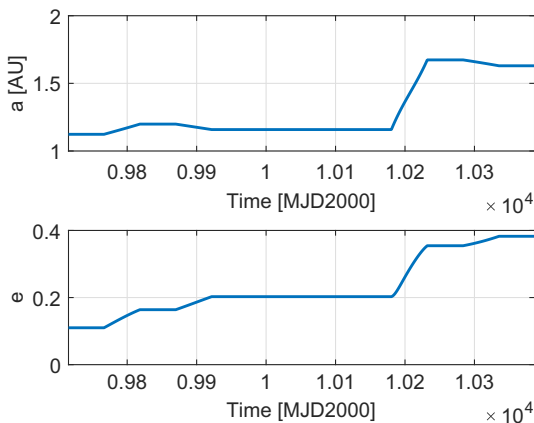


Fig. 36. Variation of semimajor axis and eccentricity during the low-thrust transfer to \mathcal{OE}_{1+2} .

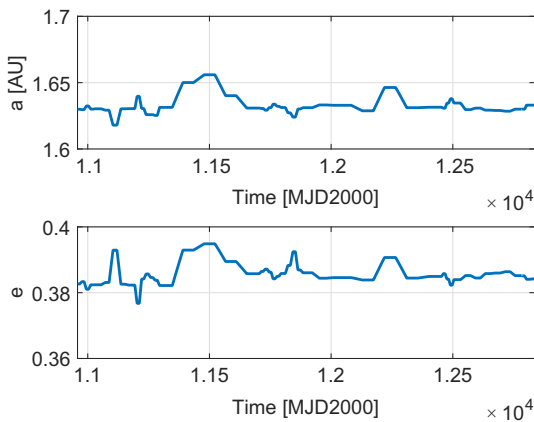


Fig. 37. Variation of semimajor axis and eccentricity during the low-thrust tour of the selected objects of Database 1 + 2.

Table 16

Summary of the main mission options for Database 1 and Database 1 + 2.

	Transfer ToF [days]	Tour ToF [days]	Total ΔV [km/s]	m_f [kg]
<i>Database 1 (4 visited asteroids)</i>				
T1	1244	865	4.9485	845.09
T2	1609	865	2.6818	912.82
<i>Database 1 + 2 (11 visited asteroids)</i>				
T1	651	1817	7.0477	786.85
T2	1382	1817	3.9125	875.40

the final mass of the spacecraft, when an initial 1000 kg spacecraft is considered. The two considered transfer options, T1 and T2, are presented. In both cases, T2 is characterised by longer transfer time but lower ΔV and, therefore, higher final mass.

5. Conclusions

The paper presented some preliminary results for a possible low-thrust tour of the main belt. A particular strategy was investigated that attempts to maximise the number of flyby's, with interesting asteroids, by traversing the main belt with a heliocentric elliptical orbit with perihelion at the Earth and aphelion at, or beyond, the main belt region. It was shown that the coupling of a binary decision tree with a novel transcription method, for optimal control, based on an asymptotic expansions of the accelerated Keplerian motion provided a range of interesting solutions to this trajectory design problem.

The analysis on the database of targets with particular scientific relevance showed that, with an estimated maximum ΔV budget of 1 km/s for the asteroid tour, 4 scientifically interesting asteroids can be visited in about five years. If the database of scientifically interesting asteroids is expanded with more than 100,000 additional objects, a total of 11 asteroids could be visited with the same upper limits on mission time and ΔV budget, but among them only 2, at most, belong to the database of scientifically interesting targets. The paper also demonstrated that with low-thrust propulsion, the tour could be completed with approximately 213 kg of propellant, within a mission time of less than 7 years, and a launch with the GLSV launcher, leaving a mass margin of 68 kg. Higher mass margins are possible allowing for longer transfer times to the main belt or using the Soyuz launcher.

It was noted that by increasing the δ tolerance on the phasing and relaxing the constraint on the estimated ΔV even longer sequences are possible with an optimised ΔV that might make the mission possible with heavier launchers. Furthermore, the launch and transfer strategy in this preliminary analysis do not include any swing-by. It is expected that a single or double fly-by of Mars could improve the number of visited asteroids, as the work of previous authors suggests. This will be the object of a future study.

Acknowledgments

This research was partially funded by Airbus Defence and Space and partially by the FP7 MSCA ITN Stardust. The authors would like to thank Dr. Pau Sanchez, at Cranfield University, the CASTAway team, and Mr. Stephen Kemble, at Airbus DS, for their support and advice.

References

- Alemany, K., Braun, R.D., Survey of global optimization methods for low-thrust, multiple asteroid tour missions. In: Proceedings of the 17th AAS/AIAA Space Flight Mechanics Meeting, January 28–February 1, 2007, Sedona, Arizona, Paper AAS 07-211.
- Bonanno, C., 2000. An analytical approximation for the MOID and its consequences. *Astron. Astrophys.* 360, 411–416.
- Bottke Jr., W.F., Jedicke, R., Morbidelli, A., et al., 2000. Understanding the distribution of near-Earth asteroids. *Science* 228 (5474), 2190–2194. <https://doi.org/10.1126/science.288.5474.2190>.
- Bowles, N., Snodgrass, C., Gibbons, A., et al., 2018. CASTAway: an asteroid main belt tour and survey. *Adv. Space Res.* 62, 1998–2025. <https://doi.org/10.1016/j.asr.2017.10.021>.
- Chen, Y., Baoyin, H., Junfeng, L., 2014. Accessibility of main-belt asteroids via gravity assist. *J. Guid. Contr. Dyn.* 37 (2), 623–632. <https://doi.org/10.2514/1.58935>.
- Di Carlo, M., Romero Martin, J.M., Vasile, M., 2017a. CAMELOT: computational-analytical multi-fidElity low-thrust optimisation toolbox. *CEAS Space J.* 2017 (September), 1–12. <https://doi.org/10.1007/s12567-017-0172-6>.
- Di Carlo, M., Romero Martin, J.M., Ortiz Gomez, N., Vasile, M., 2017b. Optimised low-thrust mission to the Atira asteroids. *Adv. Space Res.* 59 (7), 1724–1739. <https://doi.org/10.1016/j.asr.2017.01.009>.
- Di Carlo, M., Vasile, M., Minisci, E., 2015. Multi-population adaptive inflationary differential evolution algorithm. In: Proceedings of the 2015 IEEE Congress on Evolutionary Computation, 25–28 May 2015, Sendai, Japan. <https://doi.org/10.1109/CEC.2015.7256950>.
- Grigoriev, I.S., Zapletin, M.P., 2013. Choosing promising sequences of asteroids. *Automat. Rem. Contr.* 74 (8), 1284–1296. <https://doi.org/10.1134/S0005117913080055>.
- Gronchi, G.F., 2002. On the stationary points of the squared distance between two ellipses with a common focus. *SIAM J. Sci. Comput.* 24, 61–80. <https://doi.org/10.1137/S1064827500374170>.
- Gronchi, G.F., 2005. An algebraic method to compute the critical points of the distance function between two Keplerian orbits. *Celest. Mech. Dyn. Astron.* 93, 295–329. <https://doi.org/10.1007/s10569-005-1623-5>.
- Kemble, S., 2006. *Interplanetary Missions Analysis and Design*. Springer Science & Business Media, Berlin, Germany.
- Lantoine, G., Russell, R.P., 2012. A hybrid differential dynamic programming algorithm for constrained optimal control problems. Part 2: Application. *J. Optimiz. Theory Appl.* 154 (2), 418–442. <https://doi.org/10.1007/s10957-012-0038-1>.
- Millis, R.L., Wasserman, L.H., Franz, O.G., et al., 1987. The size, shape, density, and albedo of Ceres from its occultation of BD+8 471. *Icarus* 72 (3), 507–518. [https://doi.org/10.1016/0019-1035\(87\)90048-0](https://doi.org/10.1016/0019-1035(87)90048-0).
- Minton, D.A., Dynamical History of the Asteroid Belt and Implications for Terrestrial Planet Bombardment, PhD Thesis, University of Arizona, 2009. <http://www.lpl.arizona.edu/daminton/Minton_dissertation.pdf>.
- Olympio, J.T., 2011. Optimal control problem for low-thrust multiple asteroid tour missions. *J. Guid. Contr. Dyn.* 34 (6), 1709–1719. <https://doi.org/10.2514/1.53339>.
- Price, K., Storn, R.M., Lampinen, J.A., 2006. *Differential Evolution: A Practical Approach to Global Optimization*. Springer Science and Business Media, Berlin, Germany. <https://doi.org/10.1007/3-540-31306-0>.
- Rayman, M.D., Mase, R.A., 2014. Dawn's exploration of Vesta. *Acta Astronaut.* 94 (1), 159–167. <https://doi.org/10.1016/j.actaastro.2013.08.003>.
- Russell, C.T., Raymond, C.A., Ammannito, E., et al., 2016. Dawn arrives at Ceres: exploration of a small, volatile-rich world. *Science* 353 (6303), 1008–1010. <https://doi.org/10.1126/science.aaf4219>.
- Sanchez Cuartielles, J.P., Gibbons, A., Snodgrass, C., Bowles, N., 2016. Asteroid belt multiple fly-by options for M-class missions. In: Proceedings of the 67th International Astronautical Congress, IAC-2016, 26–30 September 2016, Guadalajara, Mexico. <https://dspace.lib.cranfield.ac.uk/bitstream/1826/10874/1/Asteroid_belt_multiple_flyby_options_for_M-Class_Missions-2016.pdf>.
- Shang, H., Liu, Y., 2017. Assessing accessibility of main-belt asteroids based on Gaussian process regression. *J. Guid. Contr. Dyn.* 40 (5), 1144–1154. <https://doi.org/10.2514/1.G000576>.
- Stuart, J.S., 2001. A near-Earth asteroid population estimated from the LINEAR survey. *Science* 294 (5547), 1691–1693. <https://doi.org/10.1126/science.1065318>.
- Vallado, D., 2007. *Fundamentals of Astrodynamics and Applications, Space Technology Library*. Springer-Verlag, New York, USA.
- Vasile, M., Minisci, E., Locatelli, M., 2011. An inflationary differential evolution algorithm for space trajectory optimization. *IEEE Trans. Evol. Comput.* 15 (2), 267–281. <https://doi.org/10.1109/TEVC.2010.2087026>.
- Vroom, A., Di Carlo, M., Romero Martin, J.M., Vasile, M., 2016. Optimal trajectory planning for multiple asteroid tour mission by means of an incremental bio-inspired tree search algorithm. In: Proceedings of the 2016 IEEE Symposium Series on Computational Intelligence, 6–9 December 2016, Athens, Greece. <https://doi.org/10.1109/SSCI.2016.7850108>.
- Wales, D.J., Doye, J.P., 1997. Global optimization by basin-hopping and the lowest energy structures of Lennard-Jones clusters containing up to 110 atoms. *J. Phys. Chem. A* 101 (28), 5111–5116. <https://doi.org/10.1021/jp970984n>.
- Yang, H., Li, J., Baoyin, H., 2015. Low-cost transfer between asteroids with distant orbits using multiple gravity assists. *Adv. Space Res.* 56 (5), 837–848. <https://doi.org/10.1016/j.asr.2015.05.013>.
- Zuiani, F., Vasile, M., Palmas, A., Avanzini, G., 2012. Direct transcription of low-thrust trajectories with finite trajectory elements. *Acta Astronaut.* 72, 108–120. <https://doi.org/10.1016/j.actaastro.2011.09.011>.
- Zuiani, F., Vasile, M., 2015. Extended analytical formulas for the perturbed Keplerian motion under a constant control acceleration. *Celest. Mech. Dyn. Astron.* 121 (3), 275–300. <https://doi.org/10.1007/s10569-014-9600-5>.